Comparison of Climate Variability and Mean Temperature as Expressed in Water Isotopes from Two High-Resolution Greenland Ice Cores

by

Adira Lunken

Undergraduate Honors Thesis
Department of Chemistry
University of Colorado at Boulder
Spring 2025

Defense Date: April 7, 2025

Thesis Committee:
Thesis Advisor: Tyler R. Jones (Institute of Arctic and Alpine Research)
Honors Council Representative: Jose L. Jimenez (Department of Chemistry)
Outside Reader: Jianghanyang Li (Department of Atmospheric and Oceanic Studies)

Acknowledgements

Writing an honors thesis is no small task, and I am so grateful to everyone who has helped me along the way.

First and foremost, I am deeply thankful for my advisor Dr. Tyler Jones. Tyler has gone above and beyond as an advisor, pushing me to do my best and never letting me slack off. He always believed in me, kept me on track, and spent hours editing my less-than-perfect writing to help me shape it into something far more coherent and polished. To say the least, I could not have done this without Tyler's help (and all of while he was on paternity leave, making it an even bigger thank you).

Another big thank you goes to everyone in the lab. CPL crew (Brooke, Ella, Rhys, Val, Richard, and Theo) who somehow managed to make waking up early to work in a very cold freezer for hours to cut ice, a fun experience. Melter team for always supporting each other. Special thank you to Valerie, who always supports us in cutting and melting ice, and always calmly responding to any mistakes I have made while cutting or melting ice. Thank you Kevin and Brooke, for giving me feedback and edits on my thesis as well as helping me improve my work to better impress Tyler.

Another huge thank you to my friends and family. Everyone has been so supportive and helpful throughout every step of this process. Thank you Ima and Abba for all of your unending support through everything I do in life and for always helping me grow, especially through the challenges of writing my thesis. Thank you Michelle, for being a supportive roommate and helping me so much with my defense presentation. Thank you to all my friends and family who always reminded me of what I am capable of and never doubted my ability to succeed. I am so lucky to have all of you in my life.

Lastly, thank you to my thesis committee for taking the time to read my thesis and listen to my defense.

Abstract

Ice cores contain a continuous record of past climatic conditions that can date back tens of thousands of years, and in some cases millions of years. In this study, water isotope records - a proxy for local temperature - are analyzed for the Greenland Ice Sheet Project 2 (GISP2) ice core and the East Greenland Ice Core Project (EGRIP) ice core. These records extend into the last glacial period. Spectral analysis techniques are used in climate research to observe the variability of the climate system on specific time scales (e.g. decadal, as used in this study) compared to the mean temperature over windows of time (e.g. 200 year windows, as used in this study). Understanding how temperature variability and other climate influences evolve over time compared to the mean temperature can provide insight into climatic drivers. Prior studies have shown larger amount of decadal-scale temperature variability observed during colder climates of the glacial period, which points to the potential impacts of sea ice fluctuation on climate, a hypothesis put forward by Brashear et al. (2025) based on results from the EGRIP ice core. In this study, I use new data from the GISP2 ice core to test the replicability of the Brashear et al. (2025) results. I compare the decadal-scale variability between the two high-resolution ice cores to determine if climate is expressed differently at two locations in Greenland, the ice sheet summit (GISP2) and the northeast flank of the ice sheet (EGRIP). Brashear et al. (2025) found a multi-hundred year offset between declines in decadal water-isotope variability and abrupt temperature increases in the glacial period for EGRIP. I test whether this phase offset is also present for GISP2 for two abrupt warming events, the Bolling-Allerod and the end of the Younger Dryas. I finally interpret decadal-scale variability for the deuterium excess parameter, a proxy for moisture source conditions (e.g. sea surface temperature) of the snow that falls at an ice core site and post-depositional sublimation of that snow. The two ice core sites reveal notable differences in the deuterium excess variability at certain times.

1. Introduction

The modern climate is warming, on average, but contains variations around the mean that result in heat waves and cold events that are sometimes unprecedented in the historical record. Utilizing past climate records we can contextualize the current events. Beyond the historic instrumental record, which extends only to the mid-to-late 19th century, there is limited research about high-frequency climate variability (decadal timescales or less), whereas research about mean climate change (multi-decadal and greater timescales) is abundant.

Ice core records are one way to reconstruct past climate for both the mean and variability around the mean. These cores are taken by drilling into an ice sheet and extracting cylinders of ice, usually about a meter long and with a diameter of about 10 cm. The deeper into the ice sheet an ice core is drilled, the older it will be. Trapped within that ice is a record of chemistry that provides insights into how climate has changed over years, decades, centuries, and millennia. Greenland ice core records - the topic of this thesis - can date back to over 100 thousand years before the present and contain continuous records of past climate conditions.

It is important to study both mean and variability to understand climate, because those two things may not have the same pattern of change through time. Variability is important because it describes the spread of data, or in the case of my interests, is a metric to better understand climate extremes, that is, how the ups and downs are changing through time. For example, consider the case of annual climate changes from summer to winter and back again. With small annual climate variability, seasonal temperatures remain close to the mean values, as a result of mild summers and mild winters. However, with greater variability, summers can be very hot while winters may be extremely cold. We can also consider other timescales of variability, for example, how climate shifts over a few years (interannual) or across decades. Since ice cores cannot always resolve annual variability due to signal loss for different reasons (mostly firn diffusion; Grew and Ibbs, 1952; Johnsen, 1977; Whillans and Grootes, 1985), in this study my focus will be on how climate variability changed on decadal scales in Greenland. Decadal variability is an important metric because it is a timescale humans can relate to, like asking how climate changes over the ten years some students spend in graduate or medical school.

In recent years, technology in ice core science has improved to allow for higher resolution measurements, which in turn have allowed for improved studies of past climate variability at seasonal, annual, interannual, and decadal scales (Brashear et al., 2025; Hughes et al., 2020; Jones et al., 2023; Jones et al., 2018). For example, studying how mean and variability behave across abrupt climate changes of the past (e.g. Dansgaard-Oeschger Events; Johnsen et al., 1992; Dansgaard et al., 1993; Grootes et al., 1993) provides an important understanding of what mechanisms drove these conditions, which then allows for improved modeling capabilities of Earth's climate system (e.g. Boers, 2018; Dokken et al., 2013; Li et al., 2005; Li et al., 2010; Markle et al., 2018; Petersen et al. 2013). In this study, I will use two high-resolution ice core records from Greenland to better understand decadal-scale climate variability of the past, and how that variability relates to mean temperature in Greenland. The measurements of the water isotope record of the East Greenland Ice Core Project (EGRIP) was completed within the last 5 years, whereas the record for the Greenland Ice Sheet Project (GISP2) is an ongoing ice core resampling effort to create a high-resolution record for an ice core that was originally drilled in the early 1990s. From the newly measured water isotope record of GISP2, I will present results for the available time period 8,000 to almost 19,000 years before the year 2000 CE (8-19 ka, where 'ka' means thousands of years before 2000 CE). This time period includes the late-glacial period with multiple abrupt warming events and the early Holocene. These results will be compared to those of the EGRIP water isotope record for the same time period. The rest of this thesis explains the background, methods, hypotheses, and results of my study, as well as discussion based on those results.

1.1 The Hydrologic Cycle

Water is continuously moving through Earth's climate system between the atmosphere, land, oceans, and everywhere in between. This movement of water through and between different reservoirs describes the hydrologic cycle (Bernard, 1942). The hydrologic cycle is a fundamental component of Earth's climate system which is essential to humans, as it influences various climatic and ecological processes (Chahine, 1992; Kunkel et al., 1999). For example, water evaporation and sublimation absorb solar energy, cooling the surrounding environment, while cloud condensation releases heat, regulating Earth's energy balance. Precipitation patterns affect regional vegetation and provide essential freshwater for ecosystems. Additionally, the hydrologic cycle affects surface albedo, as ice and snow reflect incoming solar radiation while large bodies of water absorb much of the solar radiation (Yang et al., 2021; Pagano and Sorooshian, 2002). These are only a few of the many factors affected by the hydrologic cycle. Understanding the movement of water across the globe is critical for assessing its role in climate change, human impacts on the water cycle, and improving predictions of future hydrological and climatic events.

Natural cycles existing on various time scales affect the hydrologic cycle, such as annual changes in solar radiation (seasons), the 2-7 year cycles of the El Niño Southern Oscillation (ENSO), and Milankovitch cycles on many tens of thousands of years time scales (Milankovitch, 1941). ENSO cycles are primarily defined by variations in Pacific Ocean surface temperatures and strength of equatorial trade winds (Timmermann et al., 2018; Gleick et al., 2013). These fluctuations influence oceanic and atmospheric circulation, driving global changes in temperature, precipitation, and other weather patterns (Bjerknes, 1969; Carrillo, 1893). Milankovitch cycles describe three parameters which cause small changes in the amount of solar insolation that Earth receives. These cycles include: (1) eccentricity, variations in the Earth's orbit around the sun (100,000 year cycles), (2) obliquity, the angle that Earth's axis is tilted (41,000 year cycles), and (3) axial precession, the direction the Earth's axis is tilted towards while traveling around the sun (26,000 year cycles; Huybers and Curry, 2006; Milankovitch, 1941). Variations in these cycles are strong drivers of long-term climate change, including triggering glacial and interglacial periods (Arthur and Garrison, 1986; Imbrie et al., 1992).

Cycles affecting the hydrologic cycle, such as the ones stated previously, are studied (1) by observing modern weather conditions such as precipitation levels, groundwater, wind patterns, and cloud formation, (for example, Bierkens, 2017; Ronghui and Yifang, 1989; Montanari et al., 2015) and (2) by studying past climate utilizing climate proxies such as those found in ice cores (for example, Bird et al., 2020; Dee et al., 2023; Pratap and Markonis, 2022) . In this study, I am interested in understanding past climates. To do so, I will use a climate proxy in ice cores that involves the measurement and interpretation of water isotopes of ice, which have been demonstrated in canonical studies to be reasonable proxies for local temperature at the locations where ice cores are drilled (Charles et al., 1994; Cuffey et al., 1995; Dansgaard, 1964; Johnsen et al., 1995).

1.2 Water Isotopes

Dansgaard (1964) was among the first to establish stable isotopes of water as a proxy for local condensation temperature, showing the relationship between the mean annual stable isotope ratios of water and the mean annual temperature and appling this relationship to ice cores. Stable isotopes in ice cores have been measured since ice coring began in the 1960s and used to study many significant climate events over the past hundreds of thousands of years (e.g. Vostok ice core; Jouzel et al., 1987).

So what is an isotope? Isotopes refer to each of two or more forms of the same element that contain equal numbers of protons but different numbers of neutrons in their nuclei and hence differ in relative atomic mass. Stable isotopologues of water are water molecules with varying numbers of neutrons present in some combination of hydrogen or oxygen atoms. The three most common naturally occurring isotopologues of water are $^{1}H_2{}^{16}O$, $^{1}H_2{}^{18}O$, and $^{1}H^{2}H^{16}O$. The most abundant form of water is $^{1}H_2{}^{16}O$ which contains the most abundant forms of hydrogen (^{1}H or protium; 99.984% of hydrogen on Earth) and oxygen-16 (^{16}O; 99.763% of oxygen on Earth). The other two isotopes of water observed in this study ($^{1}H^{2}H^{16}O$ and $^{1}H_2{}^{18}O$) contain either the second most abundant form of hydrogen, also called deuterium (D or ^{2}H) which accounts for 0.0156% of hydrogen on Earth, or it contains oxygen-18 (^{18}O; 0.1995% of oxygen on Earth; Wright, 2022).

Naturally occurring physical and chemical processes lead to the partitioning of the stable isotopes of water throughout the hydrologic cycle due to the different molecular weights of the water molecules (Gat, 1996). For example, when water evaporates, the heavier water isotopes tend to stay in lower energetic states due to their heavier molecular mass. When evaporation occurs over the world's oceans, the lighter water isotopes ($^{1}H_2{}^{16}O$) are preferentially, but not exclusively, evaporated compared to the heavier isotopes (containing ^{2}H and/or ^{18}O). The partitioning of isotopes is known as fractionation. After evaporation occurs, atmospheric circulation tends to move the water vapor poleward towards higher latitudes, and in the case of an ice sheet, water vapor also moves to higher elevations. As an air parcel encounters colder temperatures, some water vapor condenses leading to rain and snow events. As the same air parcel tends to continue on a path toward higher latitudes, the heavier isotopes are preferentially lost in each successive precipitation event. The more precipitation events that occur, causes fewer heavy isotopes to remain in the air parcel, a process known as Rayleigh Distillation (Rayleigh, 1896). Cloud condensation depends on reaching a certain temperature that is low enough to induce condensation. Since temperatures tend to become cooler as clouds move from low to high latitudes, fractionation of isotopes in an air parcel can be thought of as a proxy for the temperature gradient from the tropics to the poles. Of course, the temperature at the poles is much more variable than in the tropics, so, for polar precipitation, the polar temperature becomes the dominant lever on the high-to-low latitude temperature gradient. Put another way, as shown in prior studies, water isotopes in snowfall at the poles are largely a proxy for local temperature.

Signatures of past fractionation are preserved as the different ratios of water isotopes in the layers of an ice core. The ratio of heavy ($^{1}H_2{}^{18}O$ or $^{1}H^{2}H^{16}O$) to light ($^{1}H_2{}^{16}O$) isotopes present in the ice core sample provides insight into the past local temperature, that is, the temperature gradient from moisture origin to the poles where more negative numbers represent a larger temperature gradient or colder local temperatures. The isotopic composition is expressed in delta notation (δ) with units of parts per thousand (per mil or ‰). The isotopic composition is measured relative to the international Vienna Standard Mean Ocean Water (VSMOW). δD and $\delta^{18}O$ of an ice core sample are calculated as:

$$\delta_{\text{sample}} = \left[\left(\frac{R_{sample}}{R_{VSMOW}}\right) - 1\right] \quad (1)$$

where R is the isotopic ratio of either $^{18}O/^{16}O$ or $^{2}H/^{1}H$ in the sample or VSMOW.

Craig (1961) observed a linear relationship between the ratio of hydrogen (δD) and oxygen (δ^{18}O) stable isotopes present in natural meteoric (falling from the sky) waters and their respective latitudes. This is referred to as the Global Meteoric Water Line (GMWL). The values of δD and δ^{18}O in meteoric waters decreases linearly with higher latitude:

$$\delta D = 8*\delta^{18}O + 10 \quad (2)$$

Using this relationship, Dansgaard (1964) derived the parameter deuterium-excess (dxs) which is defined as

$$dxs = \delta D - 8*\delta^{18}O \quad (3)$$

where dxs is the y-intercept of the linear relationship between δD and δ^{18}O. Dxs is dependent on sea surface temperature, humidity, and wind speed at the moisture source origin (location of evaporation; Merlivat and Jouzel, 1979; Johnsen et al., 1989; Pfahl and Wernli, 2008), or can change if the moisture source location shifts to another region with different temperature, humidity, and wind speed conditions. Dxs is a parameter that can provide insight into past oceanic moisture conditions and how they have changed throughout time (Craig and Gordon, 1965; Merlivat and Jouzel, 1979; Pfahl and Wernli, 2014). More recent research shows that dxs also depends on conditions like sublimation of prior fallen snow at the moisture deposition site (in my case, at the ice core drilling site; Steen-Larson, 2013; Steen-Larson, 2014; Steen-Larson, 2015).

Stable isotopes of water in ice cores have been commonly used to study climate over the past hundreds of thousands of years, which can be related to other paleorecords (paleo meaning 'past') to understand changes. For example, abrupt changes in climate recorded in ice cores, along with archeological evidence, has been related to the collapse of the Akkadian empire in Mesopotamia 4,200 years ago (Weiss et al., 1993; Gill 2000; Hodell et al., 1995; Axtell et al., 2002). Volcanic ash is also preserved in ice cores and can be used to compare to temperature changes in ice cores following volcanic eruptions such as the extreme temperature decrease following the Tambora eruption in 1815 (Cole-Dai et al., 2009). Ice cores can also be used to observe temperature changes further back in time (hundreds of thousands of years ago). Using deep ice cores, temperatures and other conditions from the last interglacial period can be compared to those of the current interglacial period (Masson-Delmotte et al., 2011). These are only a few examples of the abundant amount of knowledge that can be gained by studying ice cores.

1.3 Instruments used for Measuring Water Isotopes

The traditional method used for measuring the stable isotopic composition of water is Isotope Ratio Mass Spectrometry (IRMS). This technique has been used to measure discrete water samples of about 3-5 cm for ice core analysis in the past (Gkinis et al., 2011; Gkinis et al., 2014; Gkinis et al., 2021). Measuring water isotopes with IRMS is a time consuming process that typically produces about 40-60 data points per day using one instrument, and requires separate instruments to measure hydrogen and oxygen isotopes. That is, IRMS requires the water sample to be converted to a different gas to measure either the oxygen or hydrogen isotopic ratios present (Gkinis et al., 2011). More recently, high-precision laser absorption spectroscopy (LAS) coupled with continuous flow analysis (CFA) has become the widely adopted alternative to IRMS (Jones et al., 2017a). CFA refers to melting ice, vaporizing it, and continuously injecting vapor into a laser spectrometer to measure water isotopes. CFA-LAS has many advantages, including its ability to simultaneously measure the ratio of $^{18}O/^{16}O$ and $^{2}H/^{1}H$ of the sampled water vapor, a smaller sample size than IRMS, and the ability to produce millimeter-scale resolution, as opposed to the centimeter scale measurements normally performed in IRMS (Gkinis et al., 2011).

One of the main methods of LAS used to analyze stable isotopes of ice cores is cavity ring-down spectroscopy (CRDS) which is utilized in this study. CRDS uses a series of mirrors that reflect laser pulses that detect the isotopes by comparing the extinction of a laser pulse at different frequencies in the cavity (Jones et al., 2017a). When the laser is turned off, the extinction of the laser pulse and loss of energy at different frequencies can be used to calculate water isotope values at 1 Hz (every second). The combination of fast 1 Hz measurements and the right melt rate of ice (around 3 cm/min) is what yields mm-scale water isotope measurements in ice cores, and this high data density provides the opportunity to interpret climate change of the past at the finest detail. In this study, it provides the opportunity to interpret climate variability at decadal timescales in two Greenland ice cores extending into the last ice age, more than 18,000 years ago.

1.4 High-Frequency Interpretations of Water-Isotope Variability

There are two ways to think about variability in high-resolution water-isotope records of ice cores that have been measured using LAS-CFA. The first is the simplest approach, which is to use standard deviation. The standard deviation (σ) is a measure of how dispersed the data is in relation to the mean. So, if a window of data is selected, say 500 years worth of data from some time period of the past, the $\pm 1\sigma$ standard deviation will provide a single value that represents 68.27% of values that lie within a $\pm 1\sigma$ interval of the mean. This calculation takes into account all data points. Another way to interpret variability is to isolate certain frequencies and ignore other frequencies using spectral analysis (Percival & Walden, 1993). This approach allows me to focus on decadal scale variability - the focus of this thesis - while eliminating centennial, millennial, interannual, and annual scale variability. The spectral analysis approximates data using sine and cosine waves, and from that approximation provides an estimation of amplitudes at different frequencies. I describe this in more detail in the Methods Section.

1.5 Ice Cores and the Time Periods Considered in this Study

The Earth has two major ice sheets, the Greenland Ice Sheet in North America and the Antarctic Ice Sheet at the South Pole, which both contain an archive of Earth's past climate. When snow falls in these locations it rarely melts, and instead builds up over time. The many layers of snow are compressed into ice over hundreds of thousands to millions of years. The snowfall on the ice sheet contains signatures of the climate including temperature, moisture conditions, volcanic records, and atmospheric gasses present at the time the snow fell. Ice cores are many meter-long cylinders of ice drilled from glaciers and ice sheets to study climate signatures preserved in the ice. The layers in the ice correspond to annual and seasonal snowfall over thousands of years with the youngest ice on the top and the oldest ice on the bottom. Chemical and physical differences between winter and summer snow are used to date the ice. Climate history in ice cores is preserved in climate proxies such as stable isotopes, dissolved chemicals, insoluble dust particles, and atmospheric gases in air bubbles (Barnola et al., 1987; Berner et al., 1980; Ruth et al., 2008; Delmas, 1992). Using the climate proxies in ice cores, scientists can better understand how and why climate has changed in the past which also improves predictions of how the climate will change in the future.

As previously discussed, stable isotopes of water are an established proxy for past local temperature conditions (Dansgaard, 1964). Stable isotopes in ice cores have been measured since ice coring began in the 1960s. Now, stable isotopes of water are used to study many significant climate events over the past many hundreds of thousands of years, including Dansgaard-Oeschger (D-O) events (abrupt warmings that occurred throughout the Last Glacial Period; LGP) in Northern Hemisphere ice cores and corresponding Antarctic Isotope Maxima (AIM) events in Southern Hemisphere ice cores (Jouzel, 2013).

Throughout the LGP (115-11.7 ka), Northern Hemisphere ice core records reveal many abrupt warming events known as Dansgaard-Oeschger (D-O) events, showing near interglacial (warm climate) conditions. There are 25 D-O Events ranging from 1-12 thousand years between events. D-O Events occur on millennial timescales and alternate between cold, baseline conditions (Greenland Stadials; GS) and warm periods (Greenland Interstadials; GI; Boers, 2018; Dansgaard et al., 1993). The most accepted explanation for the shift between stadial and interstadial conditions of D-O Events is changes in the Atlantic Meridional Overturning Circulation (AMOC) caused by salinity fluctuations in the Northern Atlantic (Broecker et al., 1990; Knutti et al., 2004; Peltier & Vettoretti, 2014; Stocker & Johnsen 2003). AMOC is a key component of the thermohaline circulation, a system of global ocean currents driven by differences in the ocean water's salinity, density, and temperature. Thermohaline currents transport water throughout the world's oceans over long timescales, playing a crucial role in regulating climate and distributing heat. AMOC is the main ocean current system in the Atlantic Ocean and brings warm surface waters from the tropics northward which helps warm parts of the Northern Hemisphere. AMOC strength fluctuates between strong and weak overturning during GI and GS respectively due to differences in the salinity gradient (Armstrong et al., 2022). North Atlantic sea ice is also said to be a driver of D-O Events due to its quick response to weak forcings (Brashear et al., 2025). Sea ice also largely influences the atmospheric and oceanic dynamics.

Among the most studied D-O Events is D-O Event 1, the Bølling-Allerød (BA), followed by the near-glacial conditions of the Younger-Dryas (YD). This occurred at the end of the glacial period a few thousand years before the start of the interglacial period, the Holocene. The Bølling-Allerød was an abrupt warming event beginning 14.7 ka, during which Greenland temperature rose. The BA temperatures peaked around 14.5 ka and was soon after followed by a gradual cooling climate. The YD refers to the cold period at the end of the LGP, from 12.9 ka to 11.7 ka which contained near-glacial conditions. An abrupt warming at the end of the YD marks the start of the Holocene, the current interglacial period (11.7-0 ka).

Antarctic ice cores record Antarctic Isotope Maxima (AIM) events (Ghil, 2002) which are the Southern Hemisphere counterpart to D-O Events. AIM events are recorded with much smaller temperature variations and display more gradual warming than D-O Events in Greenland (Rasmussen et al., 2016). Additionally, they are out of phase when compared to D-O Events in Greenland ice cores which is often explained by the "bipolar seesaw," an alternating ocean current phenomenon thought to control the climate variations between the two hemispheres (Broecker, 1998). The main driver of the bipolar seesaw is attributed to AMOC and heat distribution to either the northern or southern hemisphere (EPICA Community Members, 2006; Wang et al., 2015).

Both D-O and AIM Events observed in ice cores have been heavily investigated using mean temperature and climate modeling. The new ability to measure water isotopes in ice cores at high resolution enables us to analyze high-frequency climatic signals at the sub-decadal scale.

1.6 Hypotheses

Hypothesis 1: As mean temperature increases, the decadal variability in the δD and the dxs values will also increase. This would imply that more variability in δD and dxs will occur during the Holocene (warmer) than during the LGP (colder). The United States Greenland Ice Sheet Project 2 (GISP2) and the East Greenland Ice Core Project (EGRIP) are among the first deep ice cores from Greenland to be measured with continuous flow analysis coupled with cavity ring-down spectroscopy (CRDS-CFA) to produce high-frequency variability water isotope records. The decadal variability in the δD records from the ice cores can provide insight into cycles affecting changes to past temperature and the relationship between the mean and variability. The decadal variability in the dxs records can provide insight into ocean moisture source conditions or ice sheet sublimation. In this study, the mean refers to 200 year averages of δD or dxs, and for the case of δD, the 200 year average is a good approximation of local Greenland temperature.

Hypothesis 2: The two ice cores are influenced by differing climatic events and will therefore contain different patterns of decadal variability in the δD and the dxs records. This implies that a scatter plot of one record's variability vs. the other will yield a low R^2 value. Failure of this hypothesis would indicate broad climatic influences across Greenland that tended to affect both central Greenland and northeast Greenland during the Holocene and Last Glacial Period. The two Greenland ice cores are drilled at geographically different locations. EGRIP is located on an east-facing flank that may result in stronger climate influence from certain regions to the east of Greenland. Whereas GISP2 is located at Greenland's summit and is likely exposed to climate influences from a broader area, including to the west of the ice divide. The comparison of the decadal variability between the two cores can provide insight into factors influencing the two records.

Hypothesis 3: Decadal variability in δD changes at the same time as abrupt warming events in the glacial period in Greenland ice cores. If true, this would be different than the relationship previously observed for EGRIP (Brashear et al., 2025) where decadal variability changes a few hundred years prior to abrupt warming events. Hypothesis 3 thus suggests that the results of Brashear et al. (2025) are only pertinent for the eastern flank of Greenland, but do not pertain to the summit ice divide (highest point of Greenland) where the GISP2 ice core was drilled. As an example, it may be that EGRIP is detecting decadal climatic variations related to Norwegian Sea ice (a hypothesis put forward by Brashear et al., 2025), but GISP2 is detecting decadal-scale climate variability from other regions surrounding Greenland that do not have the same lead-lag relationship. A lead-lag relationship, in GISP2, will be examined by comparing when changes in mean temperature and decadal variability occur for the available abrupt warming events, the BA and end of the YD.

2. Methods

Water isotope records from two cores, the East Greenland Ice Core Project (EGRIP) and the United States Greenland Ice Sheet Project 2 (GISP2), were analyzed to observe decadal variability trends (i.e., the average amplitude of decadal variability of periods of 15-20 years) throughout the record. Both of these ice cores were obtained from Greenland and measured using continuous flow analysis (CFA) coupled with cavity ring-down spectroscopy (CRDS). The GISP2 water isotope record is currently being measured at the Institute for Arctic and Alpine Research Stable Isotope Lab (INSTAAR SIL) in Boulder, Colorado, which is part of a resampling effort of archived leftover ice from the original project campaign that occurred in the late 1980s and early 1990s. The EGRIP water isotope record was mostly measured on-site shortly after each section was drilled, but the deepest portions were measured at the Alfred Wegener Institute for Polar and Marine Research (AWI) in Bremerhaven, Germany. To determine decadal variability trends in the water-isotope records, spectral analysis techniques are used to determine the amplitudes over 15-20 year frequencies.

2.1 Study Sites and Ice Recovery

Two new high-resolution deep ice core records are being produced from Greenland ice cores to study high-frequency variability: the East Greenland Ice Core Project (EGRIP) and the United States Greenland Ice Sheet Project 2 (GISP2). EGRIP (75.38° N and 35.60° W) and GISP2 (72.58° N and 38.48° W) are both located in Greenland, but they may receive different climatic influences due to their different geographical locations, the summit compared to the flank (Grootes et al., 1993; Johnsen et al., 2001). The analyzed records of EGRIP and GISP2 can be compared to observe similarities and differences between the two ice cores to understand the impact of climate on different geographical locations.

GISP2 was drilled to bedrock over five years and completed on July 1, 1993. GISP2 is 3,053.44 m deep with a 0.132 m diameter. It was drilled using the US Polar Ice Coring Office (PICO) electro-mechanical drill (Kelly et al., 1994) with *n*-butyl acetate as drilling fluid (Grootes et al., 1993). It is located in central Greenland near the summit of the Greenland Ice Sheet. GISP2 is located near the summit of the ice sheet, so it likely receives climate influence from all regions around Greenland. GISP2 was transported to the National Science Foundation Ice Core Facility (NSF-ICF) in Lakewood, Colorado, to be further cut and distributed to labs for analysis.

EGRIP was drilled (2016-2023) on a flank (one side of the ice divide), so its water isotopes tend to be more biased to one region of Greenland's climate. It is located upstream of the Northeast Greenland Ice Stream (NEGIS) and was the first deep ice core drilled inside an active ice stream. Because of its unique location, it can provide insight into the driving mechanisms of the NEGIS by providing information about ice dynamics and post-depositional effects on the ice core (Brashear et. al, 2025). The isotope record of EGRIP was primarily measured on-site at the ice core camp shortly after each section of the ice core was drilled. The deepest portions of the ice core were shipped to AWI in Bremerhaven, Germany, where the isotopes of water were measured in a laboratory at the end of the project. in the field using the CFA coupled with Picarro L-2130 Cavity Ring Down Spectroscopy (CRDS) instrument, which is the same system used to analyze GISP2 (Jones et al., 2017a). The water isotope record for EGRIP is available in a public repository (Vaughn et al., 2022).

Only a portion of the high-resolution GISP2 water isotope record is currently available since measurements are ongoing beyond the completion of this thesis. As of writing, data is available from ~8.1 to ~18.7 ka. The EGRIP water isotope record extends from 0 to ~49.9 ka but only the time frame available for GISP2 will be analyzed in this thesis. Both ice cores are dated according to the Greenland Ice Core Chronology (GICC05; Rasmussen et al., 2014; Seierstad et al., 2014; Svensson et al., 2008). The GICC05 was transferred onto the EGRIP ice core using tie points (Mojtabavi et al., 2020, Gerber et al., 2021). Linear interpolation corresponding to NGRIP depth-age tie points was then used for additional dating constraints on the EGRIP water isotope record (Brashear et al. 2025).

2.2 Core Processing

GISP2 has been stored in NSF-ICF since 1993, when it was originally drilled. To reanalyze the ice core for a high-frequency record, ice was cut from the ice archives stored at NSF-ICF. The ice archives of GISP2 are stored by the meter in tubes in a -36 °C freezer. Bandsaws were used to cut the cylindrical meter into 100 x 1.3 x 1.3 cm ice sticks. Every break and missing piece of ice was documented for later reference. The full meter of ice was then packaged into an acrylic tube to protect the stick during transport. To transport the ice, the many acrylic tubes holding the ice sticks were placed into a cardboard box insulated with styrofoam and freezer packs to serve as a thermal buffer. These boxes were then transported to the Institute of Arctic and Alpine Research (INSTAAR) Stable Isotope Lab (SIL) at the University of Colorado, Boulder, where they are stored in another freezer until they are isotopically analyzed using the CFA system, coupled with CRDS.

2.3 Laboratory Measurements

Water isotopes were measured using a continuous flow analysis (CFA) system in conjunction with a Picarro cavity ring-down laser spectrometer (CRDS; model L2130-i; Jones et al., 2017a). The CRDS-CFA system shown in Figure 2.1 has 3 parts: melting the ice core into liquid water, vaporizing the liquid water, and then measuring the water vapor on an isotopic analyzer. First, the ice core is melted when an individual stick sits over an aluminum melt head. The temperature of the melt head is regulated by an aluminum heater block with dilute propylene glycol circulating the heater at 14.6 ± 0.1 °C. This temperature regulates the melt rate to an average of 2.5 cm min^{-1}. The melt head has a 2 mm square that channels the meltwater into a drain with tubing to move the water. Peristaltic pumps push the water through an 8 µm disposable filter followed by a 10 µm PEEK frit (IDEX A-411) to remove any ash or dust present in the ice core. Any air bubbles are then removed from the water by placing the water in an open vial. The filtered, de-bubbled water is then pulled from the bottom of the vial. A glass concentric nebulizer uses high-pressure dry air to produce a spray of water droplets about 1.5 µm into a 200 °C Pyrex vaporizing tube inside a ceramic tube furnace, which flash vaporizes the droplets. The isotopic value of the water vapor is then measured when the vapor is directed into a Picarro L2130-i analyzer and is subsampled in an open-slit (Jones et al., 2017a). The CRDS-CFA system produces high-resolution water isotope records with a resolution of ~1 mm, which is averaged to ~5 mm to account for the mixing of water in the system.

The CRDS is manufactured by Picarro. This instrument reflects laser pulses using a series of mirrors in a cavity that is filled with water vapor. By measuring the attenuation of the laser at different frequencies in both an empty cavity and one containing water vapor, the concentrations of water isotopes can be calculated (Crosson, 2008).

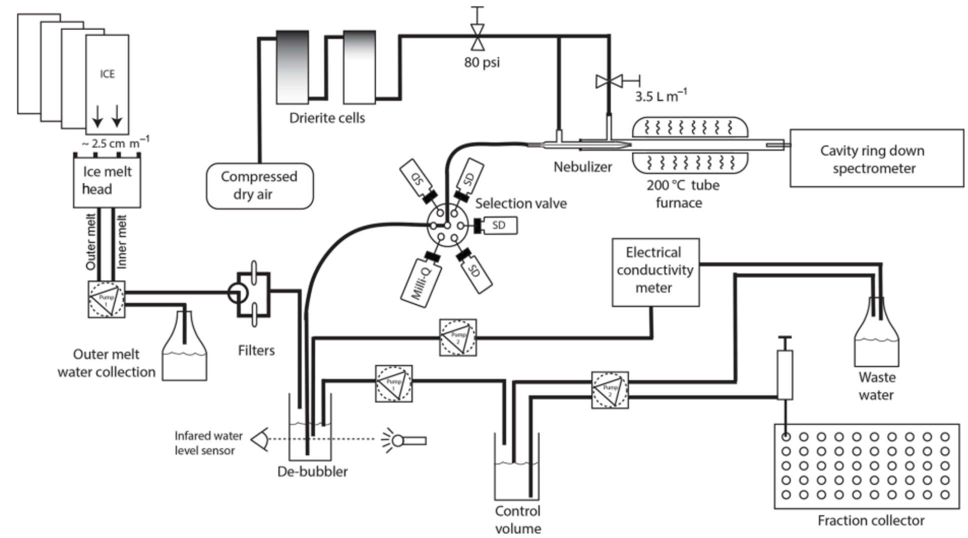

Figure 2.1: Schematic from Jones et al. (2017a) of the INSTAAR CRDS-CFA system. The schematic shows the flow of the sample from the melt head through the filter and de-bubbler. The water is pulled to the nebulizer where it is sent to the furnace to be flash vaporized. The water vapor is measured using the Picarro L-2130-i CRDS instrument.

2.4 Isotope values and standardization

The ratio of heavy to light isotopes present in an ice core sample is represented in delta notation (δ) and calculated as the parts per thousand (per mil or ‰) of the sample relative to a scientifically defined standard, Vienna Standard Mean Ocean Water (VSMOW). The International Atomic Energy Agency (IAEA) has set VSMOW to 0‰. The isotopic composition of a sample (δD or δ^{18}O) is expressed using:

$$\delta_{\text{sample}} = \left[\left(\frac{R_{sample}}{R_{VSMOW}}\right) - 1\right] \tag{1}$$

where R is the isotopic ratio of either $^{18}O/^{16}O$ or $^{2}H/^{1}H$ in the sample or VSMOW standard. δD or δ^{18}O values are standardized with VSMOW to produce consistent results globally, even though different instruments may have different sensitivities. VSMOW is used to calibrate laboratory water standards.

The CRDS-CFA system is calibrated daily and annually with laboratory isotopic water standards, which provide a range of isotopic values for δD and δ^{18}O, as shown in Table 2.1. The four water standards used daily are: Boulder standard water (BSW), Antarctic standard water (ASW), Greenland standard water (GSW), and Polar standard water (PSW). The standards are calibrated annually to IAEA primary standards: Vienna Standard Mean Ocean Water (VSMOW2), Standard light Antarctic precipitation (SLAP2), and Greenland Ice Sheet precipitation (GISP; Jones et al., 2017a).

Standards	δD	δD uncertainty	$\delta^{18}O$	$\delta^{18}O$ uncertainty
VSMOW2	0	0.3	0	0.02
SLAP2	– 427.5	0.3	– 55.5	0.02
GISP	– 189.5	1.2	– 24.76	0.09
BSW	–111.8	0.2 (1.3)	– 14.19	0.2 (0.10)
ASW	– 2 39.3	0.3 (1.3)	– 30.35	0.4 (0.10)
GSW	– 298.7	0.2 (1.3)	– 38.09	0.3 (0.10)
PSW	– 355.6	0.2 (1.3)	– 45.43	0.5 (0.11)

Table 2.1: Table of water isotope standards and their respective δD and $\delta^{18}O$ values with uncertainty in units of per mil (‰) from Jones et al. (2017a). The primary standards and their uncertainty are reported with values provided by the IAEA. The uncertainty in the laboratory standards was determined by measuring the standards with multiple isotopic analysis platforms (IRMS and CRDS), and it is reported as the average standard deviation, and in parentheses is the combined uncertainty between platforms.

Deuterium-excess (dxs) is a second-order isotope parameter that is a function of both δD and $\delta^{18}O$. Dxs is defined as:

$$dxs = \delta D - 8*\delta^{18}O \tag{2}$$

which is derived from the Global Metoric Water Line (GMWL; Dansgaard, 1964).

2.5 Spectral Analysis

To observe variability in high-resolution water isotope records, this can be done by either calculating the standard deviation or spectral analysis. Standard deviation (σ) is the simpler approach which measures ±1σ from the mean value. This calculates how far the majority (68.27%) of values are dispersed from the mean value. The other more complex method to observe variability is spectral analysis. This method uses sine and cosine waves to fit the data over specific frequencies (such as decadal frequencies as used in my analysis) and estimate the amplitude over the observed frequency. Over many windows of data, changes in amplitudes, or the variability, for a specific frequency can be observed.

Variability and mean temperature do not always change together in time, called a phase offset. It is important to document these situations since it can provide insight into climate drivers. A phase offset has been observed previously by Brashear et al. (2025) in EGRIP and Jones et al. (2018) in an ice core from West Antarctica. Figure 2.2 illustrates an example, using synthetic data, of how variability and mean temperature can change separately over time in climate data.

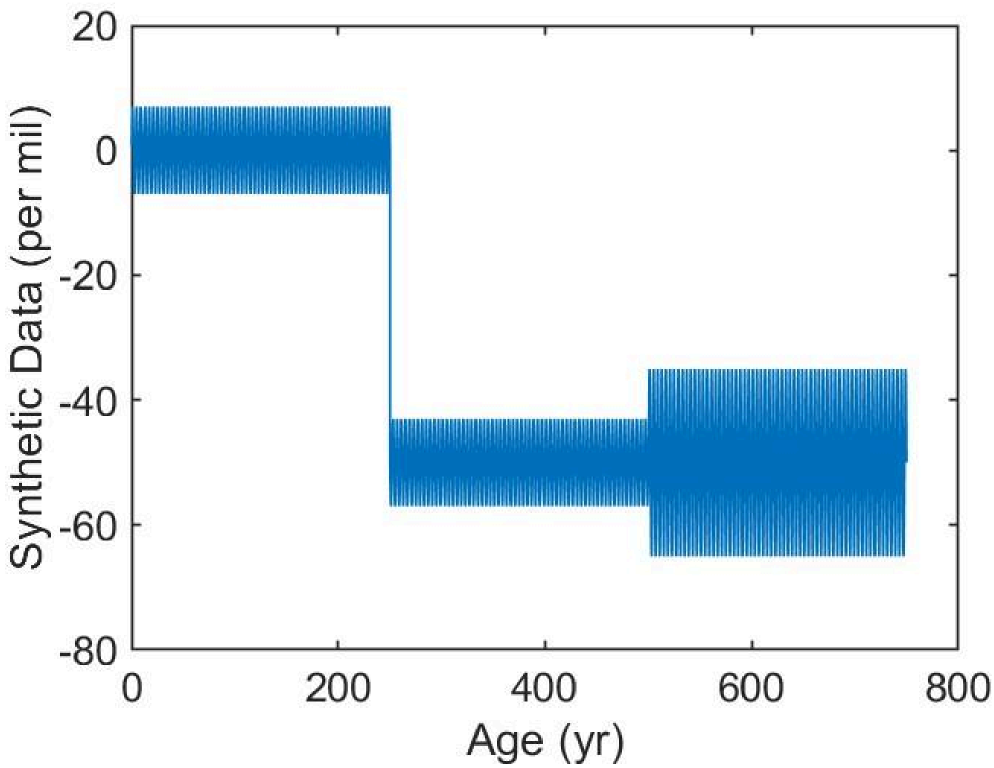

Figure 2.2: Synthetic ice core data (‰) versus age (yr) to show a change in the mean at 250 yrs followed by a change in variability (but not the mean) at 500 yrs. This highlights two instances where changes in the mean and variability are not coupled together in time. Although difficult to see, the data is plotted as repeating sine waves (frequency = $1yr^{-1}$) to represent the annual fluctuations in temperature with seasons. The average y-axis value is 0‰ from 0-250 yrs when the mean temperature, represented by the synthetic data, changes to -50‰. The variability in the data is the spread of the sine wave. From 0-250 yrs the sine wave oscillates from +7‰ to -7‰, so the standard deviation is ±4.95‰. After the mean value changes around 250 yrs the data then oscillates from -43‰ to -57‰. The standard deviation is still ±4.95‰. This remains until around 500 yrs when the sine wave is larger and oscillates between -35‰ to -65‰ causing the standard deviation to increase to ±10.6‰, but the mean stays the same. This is one example of how the mean and variability can have a phase offset, which is the difference in time between the large shift in the mean and the variability change calculated as 500 yrs - 250 yrs = 250 yr phase offset.

To observe variability over specific frequencies spectral analysis was performed in MATLAB. Spectral analysis techniques, such as Fast Fourier Transform (FFT), observe the average amplitude over a window of time for all frequencies. Sine and cosine waves are used by the software to fit the variability in the climate data, over a specific window of time, for thousands of frequencies from less than a year to centuries. Over the designated window of data, the FFT creates a spectrum with the average amplitude from the fit of the sine or cosine waves at the respective frequency. Changes in amplitude over time can be observed by plotting the amplitude of the chosen frequency (or averaged over a band of frequencies) for each consecutive window of time. Figure 2.3 shows synthetic climate data created from four sine waves added together. This illustrates how variability can be very difficult to interpret visually, and may even look random, when in fact the signal contains very specific frequencies and amplitudes as can seen in the bottom plot.

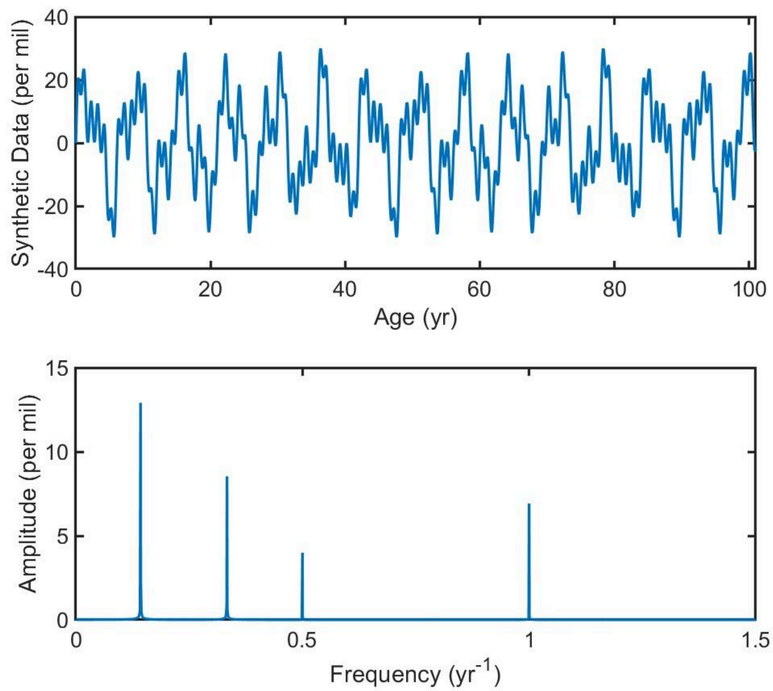

Figure 2.3: (Top) Synthetic climate data (‰) made with multiple sine waves added together plotted against the age (yr). **(Bottom)** Fast Fourier transform is used to analyze the data and find the amplitudes (‰) for each frequency (yr^{-1}).

The multi-taper method (MTM) of spectral analysis (Huybers, 2021; Percival & Walden, 1993) is often used to calculate the relative amplitudes of ice core data and other climate proxy data. An MTM is similar to an FFT but, instead of amplitudes, the MTM provides the spectral power density as a function of frequency. This power density reflects the relative strength of the frequency components within the original signal. MTM preferentially analyzes the data by minimizing spectral leakage (Huybers 2021). Put more simply, MTM can account for sine and cosine waves that are not stationary, that is, they come and go within a window of time. Earth climate is known to be non-stationary. The EGRIP and GISP2 δD and dxs records were analyzed using a 200 year window with a 20 year timestep. This provides a large enough window that adequate repetitions of the decadal signals occur, allowing for a precise estimation of the power density (amplitudes). An example power density plot is shown in Figure 2.4 for the 14-13.8 ka window of time.

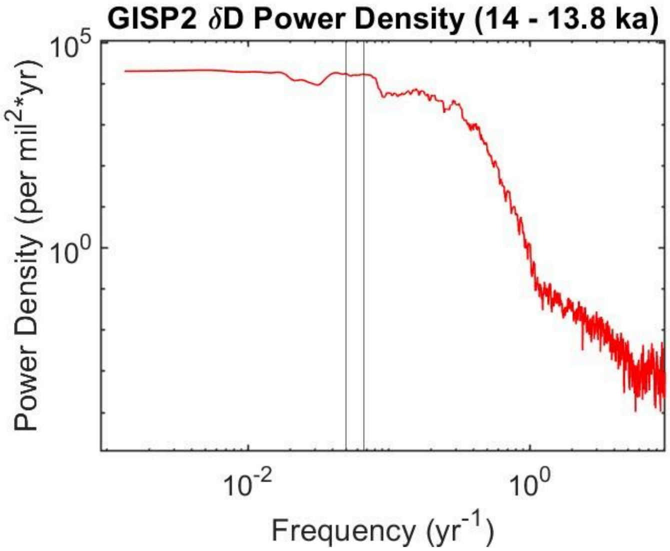

Figure 2.4: An example plot of power density (per mil^2*yr) vs. frequency (yr^{-1}) over a 200 year window of time from 14-13.8 ka for the GISP2 δD record. The vertical lines designate the frequency band of 15-20 years that is not affected by diffusion and used for analysis in this study.

As shown in Brashear et al. (2025), the variability over a 15 to 20 year frequency is not affected (or minimally affected) by diffusion at EGRIP. Those same results are pertinent for GISP2, since both cores have similar accumulation rates and temperature. Accumulation and temperature are the two primary controls on diffusion (Jones et al., 2017b). Diffusion is a result of water molecules spreading out in the air pathways present in the firn layer (Grew and Ibbs, 1952; Johnsen, 1977; Whillans and Grootes, 1985). The firn layer is the upper ~50-90 m of the ice sheet where the snow has not yet been fully compacted into ice. While diffusion is beyond the scope of this thesis, a spectral analysis plot can be used to determine the effects of diffusion by fitting a Gaussian curve to the spectral data (Jones et al., 2017b), which yields a standard deviation value (also known as a 'diffusion length'). With a diffusion length, a correction to the data can be applied to remove the effect of diffusion (Jones et al., 2018), leaving an estimate of the original climate variability before diffusion occurred.

As done in prior studies (Brashear et al. 2025), I use the mean δD value within a 200 yr window to represent the mean local temperature of that time period. The δD value is a good approximation of local temperature at centennial and greater timescales. I also computed the average decadal variability (i.e. the mean amplitude of 15-20 yr signals) of the δD values, which is more representative of both local temperature and regional atmospheric circulation anomalies that might alter the temperature gradient from moisture source (i.e. a lower latitude ocean region) to deposition site (i.e. the ice core drilling site). Finally, I calculated the average decadal variability of dxs values, which provides information about moisture source conditions (sea surface temperature, relative humidity, wind speed) or sublimation at the ice sheet surface. The dxs decadal variability is currently not well understood, and the results presented in this thesis are a first step towards improving our understanding.

3. Results

The stable isotopes of water for the East Greenland Ice Core Project (EGRIP) and the United States Greenland Ice Sheet Project 2 (GISP2) were both measured with CRDS-CFA to produce high-resolution isotope records. EGRIP was drilled on the flank of the Greenland ice sheet (to the east of the ice divide). The isotope record of EGRIP was primarily measured on-site at the ice core camp from 2017 to 2023, shortly after each section of the ice core was drilled. However, the deepest portions of the ice core were shipped to AWI in Bremerhaven, Germany, where they were analyzed in a laboratory at the end of the project. GISP2 is located at the summit of the Greenland Ice Sheet, where it may record different climatic influences than EGRIP. Since GISP2 was originally drilled and measured in the early 1990s, the stable isotopes of water are currently being remeasured using archived ice stored at the National Science Foundation Ice Core Facility (NSF-ICF). High-resolution records, and by extension, those that capture high-frequency variations (such as decadal variability), allow for insights into how climate variability changes in relation to the mean temperature. The EGRIP and GISP2 records of δD and dxs values were analyzed using the multi-taper method (MTM) of spectral analysis (Huybers, 2021) as discussed in Methods to observe changes in decadal (15-20 yr) variability of the records for 200 yr windows, with 20 yr timesteps between windows, for time periods ranging from 8.1 to 18.7 ka (thousands of years before the year 2000 CE). The difference in geography between the two Greenland ice cores provides the opportunity to determine if the results are replicable (Grootes et al., 1993; Johnsen et al., 2001).

3.1 GISP2 δD Record

The raw GISP2 δD record (Figure 3.1) shows a water isotope record consistent with other ice cores from Greenland showing the same glacial to interglacial pattern. Since the resampling of GISP2 is currently ongoing, only high-resolution data from ~8.1-18.7 ka is currently available for GISP2. The Last Glacial Period (LGP) appears in this record from before 18.7 ka until about 11.7 ka which marks the beginning of the Holocene, seen as the isotope values become less negative. The colder temperatures of the mid-glacial period, from before ~14.7 ka, are reflected with the lower δD isotope values ranging mainly between -345‰ and -275‰. The abrupt warming signature of the Bolling-Allerod (BA) is observed in this record around 14.7 ka. This is the second to last abrupt warming that occurred before the start of the Holocene, and the BA is also often referred to as D-O Event 1. At the start of the BA, the average δD value rises from fluctuating around -310‰ before the BA to then fluctuating around -280‰ at the peak of the BA occurring around 14.5 ka. The high δD isotope values at the peak of the BA are a signature of the near interglacial temperatures during this time. As observed here, and is consistent with other D-O Events, gradual cooling follows the abrupt warming of the BA as seen by a decrease in the δD values. At the end of the LGP, during the Younger Dryas (YD), a cold period is observed in the record from about 12.9-11.7 ka, as the δD values are again lower. Similar to during the glacial period at the beginning of this record, the end of the LGP has δD values which fluctuate mostly around -310‰ and vary just below -350‰ to just above -290‰. The glacial period ends around 11.7 ka as the δD values increase during an abrupt warming, marking the start of the Holocene. The abrupt warming at the end of the YD is sometimes called D-O Event 0. After this abrupt warming, the δD values generally fluctuate between -300‰ to -240‰ from 11.7 to 8.1 ka. The higher δD values are signatures of the warmer climate of the interglacial period. During the Holocene, a climate optimum is observed around 9 ka, with δD values varying mostly between -285‰ and -250‰.

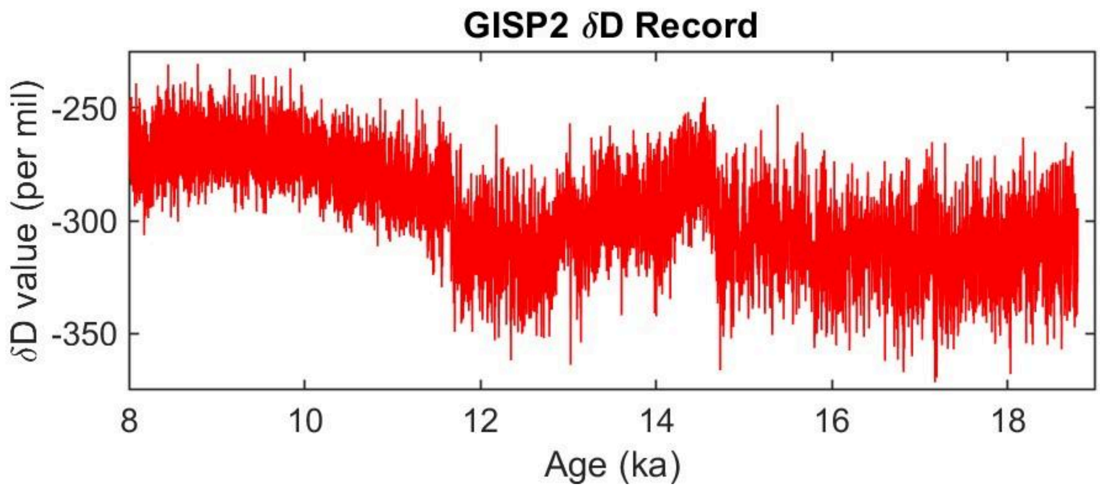

Figure 3.1: Plot of GISP2 δD (‰) vs. Age (ka).

3.2 GISP2 Deuterium Excess Record

Deuterium excess (dxs) is mainly influenced by the conditions at the moisture origin point including sea surface temperature, humidity in the air above the sea, and wind speed. It can also be affected if the moisture origin of the precipitation changes or by conditions at the deposition site. The dxs record is a derived parameter calculated from the relationship between δD and δ^{18}O using equation 2 as explained in Methods. Dxs is a complex parameter and therefore difficult to understand.

The dxs record for GISP2 (Figure 3.2) is among the highest resolution Greenland dxs records to be analyzed. Throughout the record, shifts in the dxs value correlate to significant climatic events. The most distinct shift occurs at the start of the BA around 14.7 ka. Before the BA the dxs values varied mainly between 5‰ to 10‰ from 18.7-17 ka, and then mostly between 7‰ and 12‰ from 17-14.7 ka. At the start of the BA, the dxs record declines and varies between 2‰ and 6‰ followed by a rise over the next many hundreds of years. The dxs record during the YD (12.9-11.7 ka) is again higher with values varying mostly between 7‰ and 13‰. At the start of the Holocene (11.7 ka), the dxs values decline and vary between 5‰ and 9‰. From 11.7-8.1 ka, the dxs values gradually increase to fluctuate between 7‰ and 11‰ by 8.1 ka.

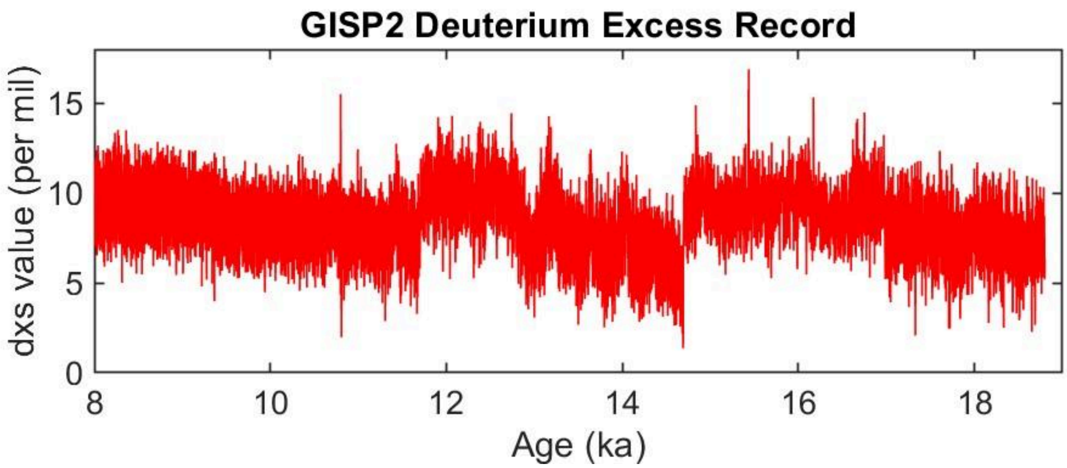

Figure 3.2: Plot of the GISP2 dxs (‰) vs. Age (ka).

3.3 GISP2 Relative Amplitudes of Decadal Signals

The decadal variability in the water isotopes, δD and dxs, are determined throughout time to observe how the variability changes. The MTM spectral analysis was performed in MATLAB as described in Methods. To do so, the amplitudes for 15-20 yr frequencies over a 200 yr window of the records were calculated with a 20 yr timestep. The results are normalized by dividing the entire decadal variability record by the value in the most recent data window, i.e., the variability from 8.1-8.3 ka (which has a relative amplitude of 1). The 15-20 yr frequency was chosen since it is not affected by diffusion, as discussed earlier.

3.3.1 GISP2 δD Decadal Variability

The relative amplitudes for GISP2 decadal variability (Figure 3.3 bottom) are compared with the mean temperature (δD mean value in each 200 year window). The variability throughout the record fluctuates from 0.5 to 10 times (0.5-10x) as much decadal variability compared to the first window analyzed from 8.1 to 8.3 ka. Overall the LGP contains larger decadal variation than the Holocene. The oldest part of the record (18.7-14.7 ka) contains relative amplitudes that fluctuate between 4-10x. At the start of the BA (14.7 ka), a large decrease in decadal variability occurs where the relative amplitude drops to 1.3x around the time of the BA. During the YD (12.9-11.7 ka), the decadal variability again rises. The relative amplitudes during the YD range from about 3-9x. This is similar to the larger variability seen prior to the BA. At the start of the Holocene, the decadal variability decreases significantly to range between 1-3x. Around 10.3 ka the variability decreases even more to fluctuate only between 0.5-1.5x for the rest of the available record.

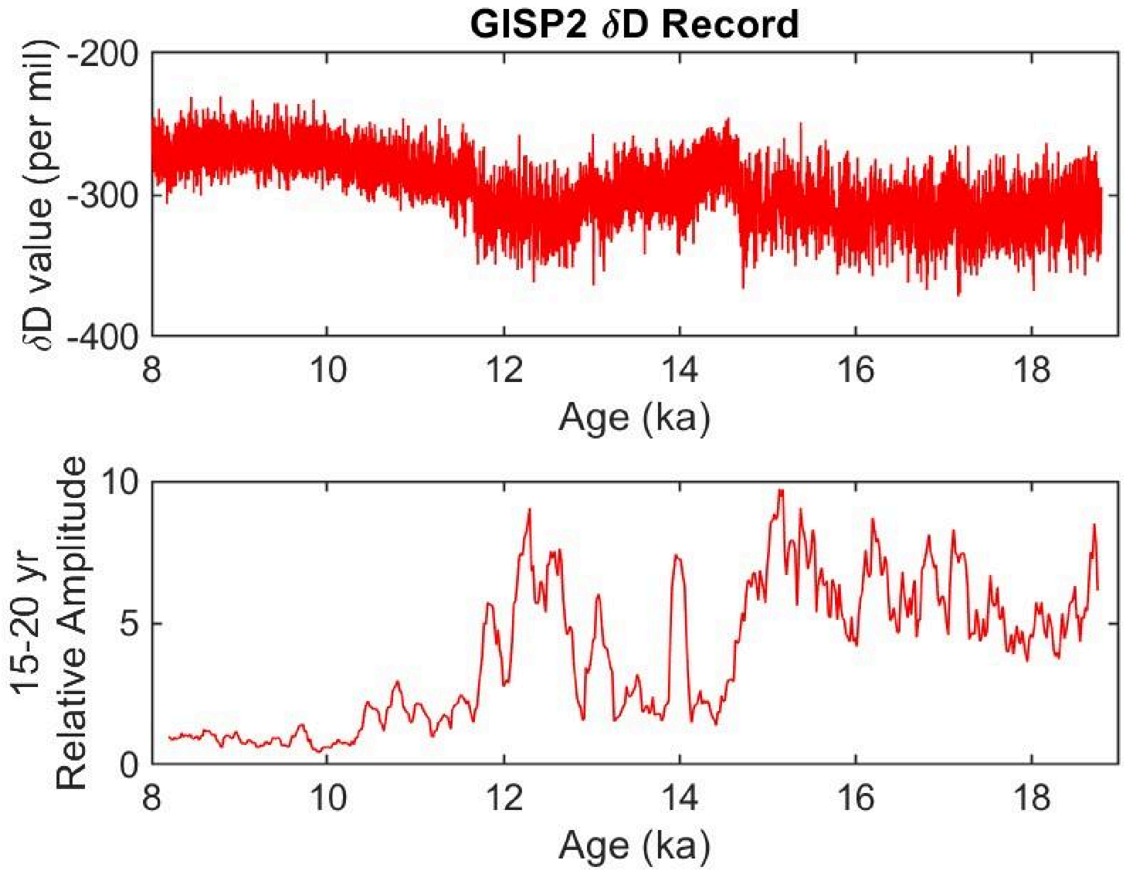

Figure 3.3: Plots of GISP2 δD water isotope data and decadal amplitudes. **(Top)** δD (‰) vs. Age (ka). **(Bottom)** 15-20 year relative amplitudes vs. age (ka) calculated for 200 yr window sizes and 20 yr timesteps, where relative amplitudes are calculated from the average power density value within the 15-20 yr frequencies for each respective window of data and all amplitudes were then divided by the amplitude of the first window of data (8.1-8.3 ka) to calculate the relative amplitudes of the record.

3.3.2 GISP2 Dxs Decadal Variability

A novel part of this study was to observe the decadal variability of the dxs values throughout the record. The relative amplitudes GISP2 dxs record (Figure 3.4 bottom) are compared to the major climatic events at the time. The decadal variability of dxs ranges from 0.5 to 5 (0.5-10x) times as much variability as the first window of data (8.1-8.3 ka). For the entire record analyzed, generally, larger decadal variability occurs during the colder Last Glacial Period and Younger Dryas, and less decadal variability occurs during the warmer Bolling-Allerod and Holocene. The older portion of the LGP present in this record (18.7-14.5 ka) contains significant variations in decadal variability with portions of less variability dropping to almost 1x in some parts, and then peaks of variability reaching almost 5x. The variability then decreases to around 1 at the peak of the BA (14.5 ka). As the climate cools after the abrupt warming of the BA, the variability starts to increase again ranging from 1-3x until about 12.6 ka. During the YD, the variability contains two distinct increases to about 5x variability occurring between 12.9-11.7 ka. Throughout the Holocene shown in this record (11.7-8.1 ka), the relative amplitudes consistently fluctuate within 0.5-2x.

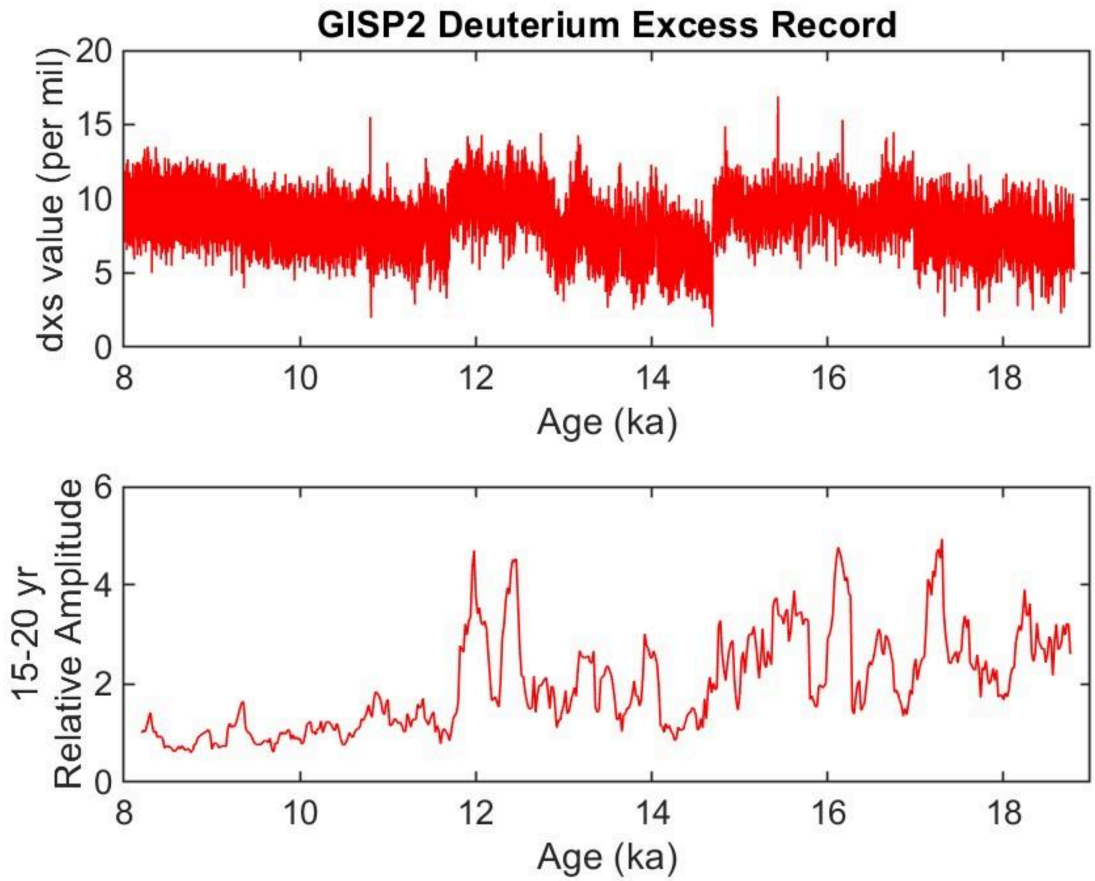

Figure 3.4: Plots of GISP2 dxs isotope data and decadal amplitudes. **(Top)** Dxs (‰) vs. Age (ka). **(Bottom)** Relative amplitudes vs. Age (ka) were calculated for 200 yr window size and 20 yr timestep, where average amplitudes are calculated from the average power density value within the 15-20 yr frequencies for each respective window of data and all amplitudes were then divided by the amplitude of the first window of data (8.1-8.3 ka) to calculate the relative amplitudes of the record.

3.4 EGRIP Relative Amplitudes of Decadal Signals

The decadal variability in the δD and dxs records of EGRIP were also analyzed in the same way as for GISP2. EGRIP provides the opportunity to compare the results for GISP2 to a previously measured record. Although the entire EGRIP record dates back to ~49.9 ka, only 8.1-18.7 ka was analyzed as that allows for a direct comparison of records over the same time periods. EGRIP δD variability was previously analyzed by Brashear et al. (2025), but the previous analysis did not include dxs variability which is included in this thesis. Here I will show the results of the spectral analysis of EGRIP δD and dxs decadal variability since variability in the EGRIP water isotope records are used for further analysis.

3.4.1 EGRIP δD Decadal Variability

Throughout the record, the variability has varying trends and amplitudes as seen in Figure 3.5, bottom plot. During the glacial period from 18.7-14.7 ka the decadal variability fluctuates from 2-7x. From ~14.7-13.5 ka, during the BA, the variability decreases fluctuating only between 1-3x. The variability increases slightly around 13.5 ka, fluctuating around 2-4x, during the YD. Throughout the Holocene, the decadal variability in temperature fluctuates around 1x. This variability is small and consistent compared to variability during the LGP.

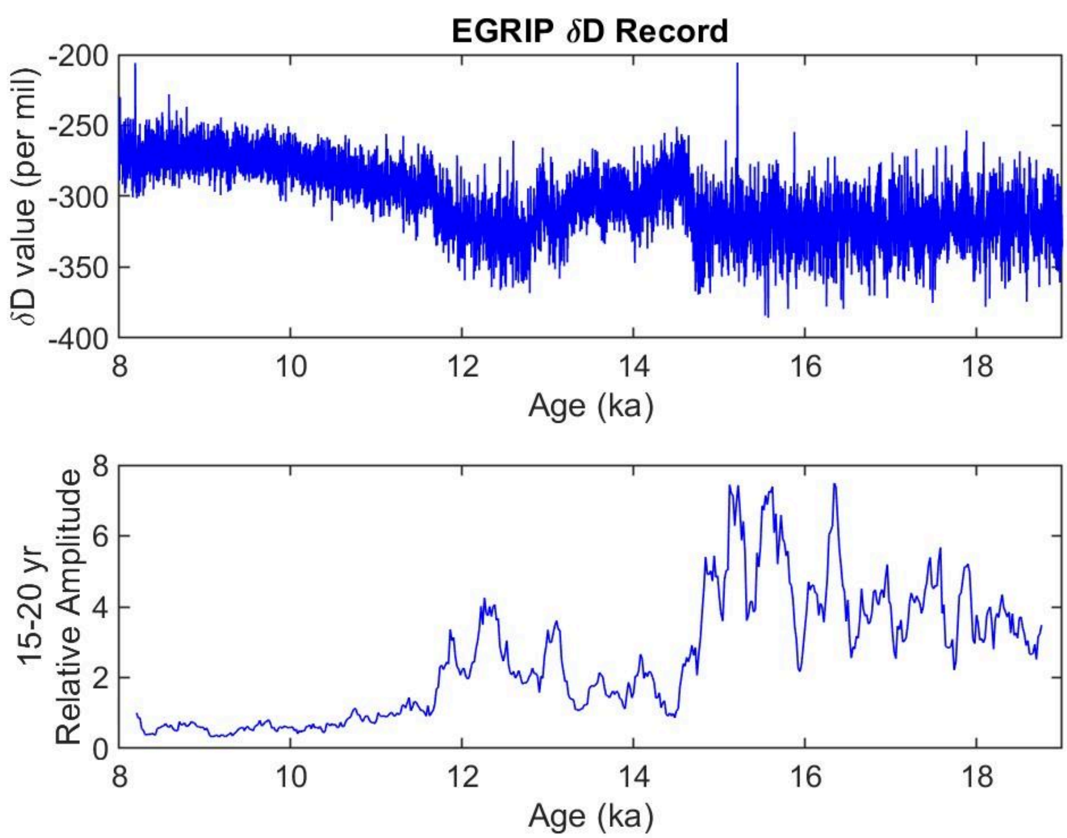

Figure 3.5: Plots of EGRIP isotope data and decadal amplitudes. **(Top)** δD (‰) vs. Age (ka). **(Bottom)** Relative amplitudes vs. age (ka) calculated for 200 yr window size and 20 yr timestep, where average amplitudes are calculated from the average power density value within the 15-20 yr frequencies for each respective window of data and all amplitudes were then divided by the amplitude of the first window of data (8.1-8.3 ka) to calculate the relative amplitudes of the record.

3.4.2 EGRIP Deuterium Excess Decadal Variability

The dxs record for EGRIP (Figure 3.6 Top) is the highest resolution and longest continuous Greenland dxs record to be analyzed to date, although the GISP2 record will eventually extend even further back in time (measurements were completed after the publication of this thesis). A novel part of this study was to look at the decadal variability of the dxs values throughout the EGRIP and GISP2 records. The relative decadal variability of EGRIP is shown in Figure 3.6, bottom plot. The relative amplitudes during the LGP, 35-11.7 ka, appear to fluctuate somewhat randomly between 1-9x. Toward the end of the glacial period, a decrease in variability occurs from about 15-13 ka during which the amplitudes only range from ~1-4x. This is around the time of the Bolling-Allerod. The dxs decadal variability then increases, around the time of the YD from ~13-11.7 ka, fluctuating between ~2-6x during this period. During the Holocene, 11.7-8.1 ka, the relative amplitudes fluctuate around 0-2x.

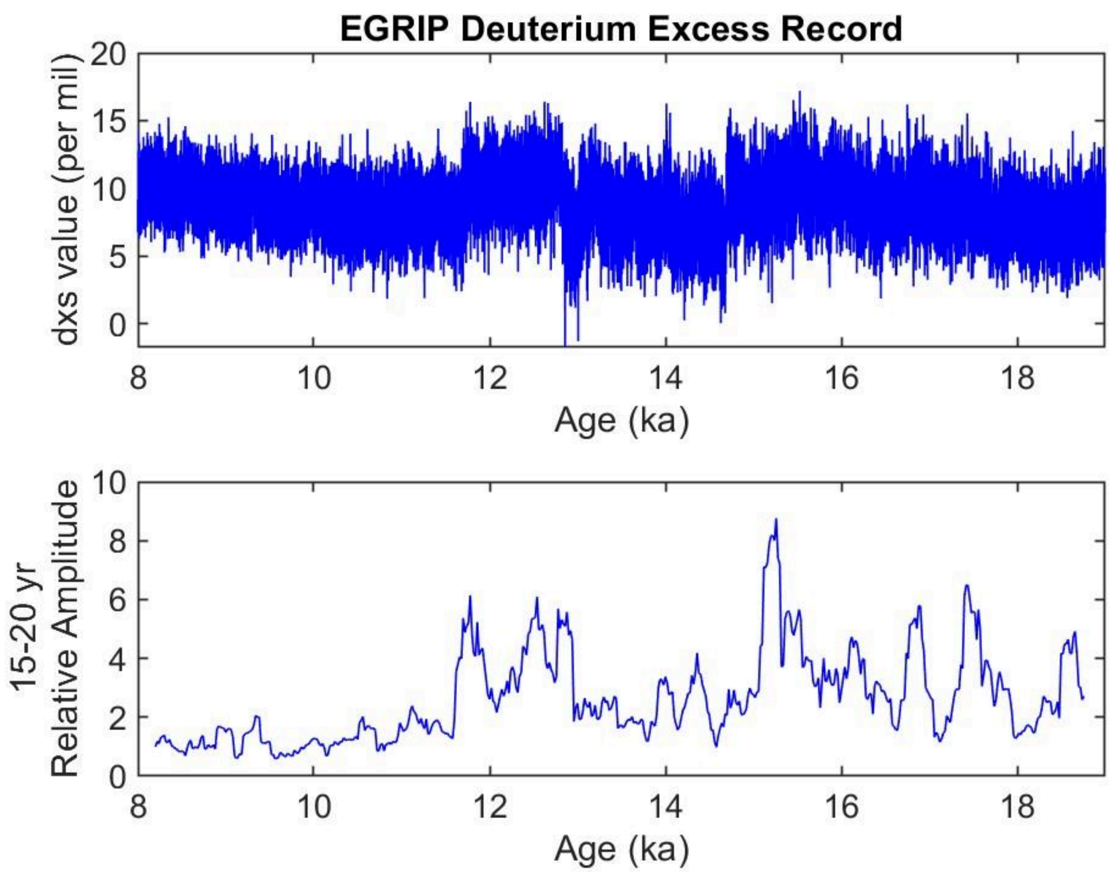

Figure 3.6: Plots of EGRIP deuterium excess isotope values and decadal amplitudes. **(Top)** Dxs (‰) vs. Age (ka). **(Bottom)** Relative amplitudes vs. Age (ka) calculated for 200 yr window size and 20 yr timestep, where average amplitudes are calculated from the average power density value within the 15-20 yr frequencies for each respective window of data and all amplitudes were then divided by the amplitude of the first window of data (8.1-8.3 ka) to calculate the relative amplitudes of the record.

3.5 Comparison of Isotope Decadal Variability and Mean Temperature

To observe the relationship between temperature and variability in temperature (δD) or variability in dxs. The decadal variations in water isotopes are calculated as explained previously with the average amplitudes of 15-20 yr frequencies over a 200 year window. All the values are then divided by the first window of time (8.1-8.3 ka, which receives a relative amplitude of 1) to calculate the relative amplitudes. These values are plotted against the average δD value over that window of time, to represent mean local temperature (a good approximation of local temperature at centennial and greater timescales). Linear regressions were used to find the R^2 and P-values which quantify the linear relationship of the two parameters throughout the observed period of time. The scatter plots in Figures 3.7 and 3.8 include only the variability records over the period of time available for GISP2 (8.1-18.7 ka).

To understand how different mean temperatures (the independent variable) cause changes to the variability in the temperature or dxs (the dependent variable) linear regressions were used to fit the data. The amount of linear relationship that exists within a data set is quantified with the R^2 value. First, a linear fit of the data creates a 'model' to represent the average relationship between the temperature and the amount of variability in decadal temperature (or dxs value) for the climate system. The R^2 values represent a percentage showing how well the model (the linear fit representing how variability changes with temperature) explains the data. For example, if variability increases linearly with temperature to form a straight line with no exceptions in the climate system then the R^2 value will be 1 (i.e. the linear fit can be used 100% of the time to calculate the decadal variability from the average temperature). Because of randomness and natural variability in the climate system, it is more likely to produce a lower R^2 value such as 0.6, which means the model (linear fit) explains the relationship of the data for only 60% of the data. Furthermore, a P-value is calculated to test the null hypothesis that the relationship is due to random noise. If a statistically significant relationship between the mean temperature and variability in water isotope values exists then the P-value must be below 0.05 to show the relationship is not a result of random noise.

3.5.1 Decadal Variability of Temperature Compared to Mean Temperature

The GISP2 record, as the main focus of this thesis, contains an overall trend of increasing decadal variability with lower temperatures, i.e. more negative δD values. For the GISP2 record, warmest δD values, higher than -280‰, have relative amplitudes below 2x. The opposite is true for colder δD values, values less than -315‰, containing variability ranging from 4-9x. This relationship is supported by the large R^2 value of 0.6844 for the entire GISP2 record, which represents the linear fit's ability to predict the variability from temperature 68% of the time. The entire GISP2 record also contains a p-value of 0.000 which suggests that this data contains a statistical relationship. The GISP2 record was divided between two time periods: 1) the Holocene (11.7-8.1 ka) and 2) the Last Glacial Period (LGP; 18.7-11.7 ka). Both of these time periods contained some relationship between increasing variability with lower temperatures, as observed over the entire GISP2 record. Both time periods contain a p-value of 0.000 showing that the data sets contain some statistical relationship. The R^2 value for the Holocene was 0.5251 which is higher than the R^2 value for the LGP of 0.3053. It should also be mentioned that with colder temperatures the relative variability covers a larger range (e.g. 3-9x variability at -310‰) whereas with warmer temperatures, the variability fluctuates much less (e.g. 0.5-1.5x variability at -265‰. The EGRIP record over the same time period as that available for GISP2 (8.1-18.7 ka) produced similar results. An overall inverse relationship between decadal variability in temperature and mean temperature exists in the record.

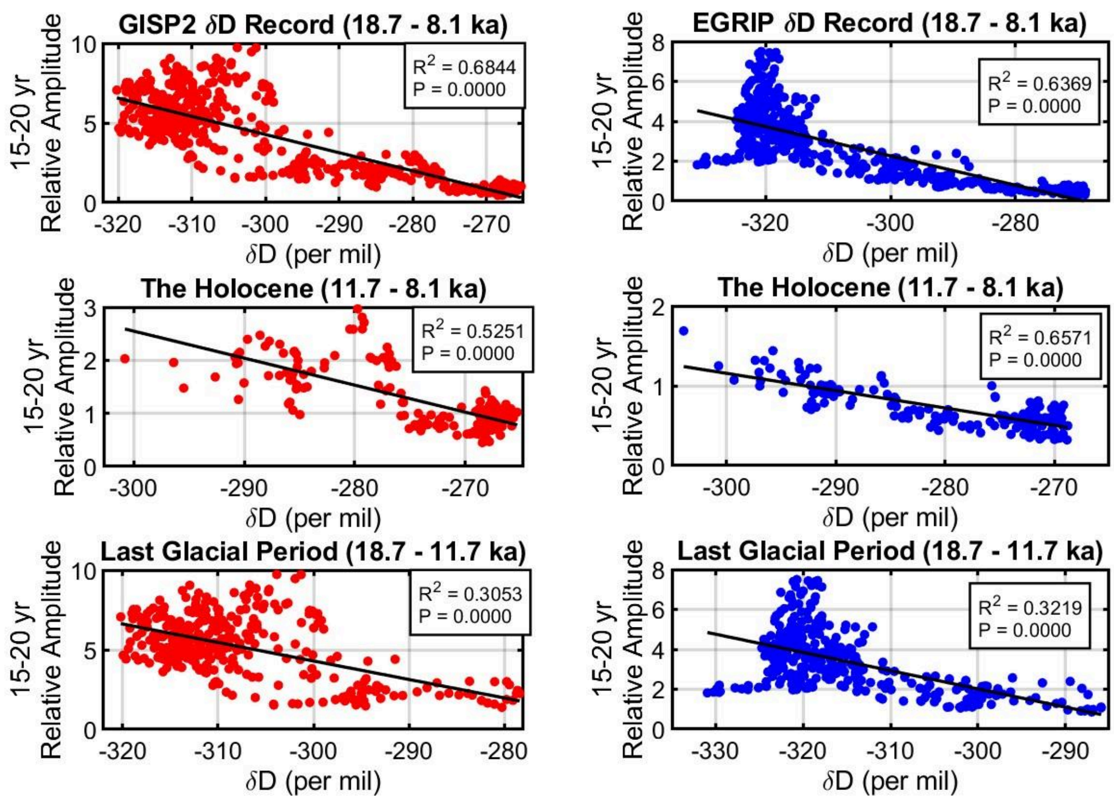

Figure 3.7: Plot of relative variability for δD isotopes over a 15-20 yr frequency versus the mean δD isotope value (‰) over the respective window (200 yr window, 20 yr timestep). All plots contain an R^2 value and p-value that were calculated using linear regressions for the data. **(Top left)** GISP2 data from 18.7-8.1 ka. **(Top right)** EGRIP data from 40-0 ka. **(Middle left)** GISP2 data from 11.7-8.1 ka during the Holocene. **(Middle right)** EGRIP data from 11.7-0 ka during the Holocene. **(Bottom left)** GISP2 data from 18.7-11.7 ka, during the LGP. **(Bottom right)** EGRIP data from 40-10 ka during the LGP.

3.5.2 Decadal Variability of Deuterium Excess Compared to Mean Temperature

The relationship between decadal variability in deuterium excess (dxs) is observed compared to the mean temperature (mean δD value over the 200 yr window) in Figure 3.8.

Deuterium excess decadal variability contains an inverse relationship to temperature. At warmer temperatures, above -270‰, the amount of decadal variability in dxs fluctuates from about 0.5-1.7x. At colder temperatures, above -310‰, the relative variability fluctuates between 1-5x. Over the entire GISP2 record the R^2 value is 0.5493 for GISP2. This shows some relationship between the two variables, but the linear fit only holds true for about half of the time. The p-value of 0.000 agrees that some statistical relationship between the mean temperature and variability in dxs exists. When the GISP2 record is divided between the LGP (18.7-11.7 ka) and the Holocene (11.7-8.1 ka), the linear fit for either scatter plot describes the relationship more poorly than over the entire record. The p-values over both time periods are 0.000, which supports some correlation between the values (i.e. they are not all randomly distributed). The Holocene contains an R^2 value of 0.2989 and the LGP contains an R^2 value of 0.2136. The low R^2 values mean that the linear relationship is not a good model for the plots over these time scales.

Similar results are observed for the EGRIP records. The entire record contains an R^2 value of 0.4555, similar to that of the entire GISP2 record, showing some relationship between dxs decadal variability and mean temperature. When the EGRIP record is split between the glacial (18.7-11.7 ka) and interglacial period (11.7-8.1 ka), similar results are obtained to those of GISP2. Notably, a small relationship exists between increasing temperature and decreasing variability. The Holocene contains an R^2 value of 0.3478, and the LGP contains an even smaller R^2 value of 0.1430. The low R^2 values of both records support the minimal relationship that exists when the records are split between the two. The p-values for all of the EGRIP records are 0.000 which shows some statistical relationship between the decadal variations in dxs and mean temperature exists, even if the relationship is small.

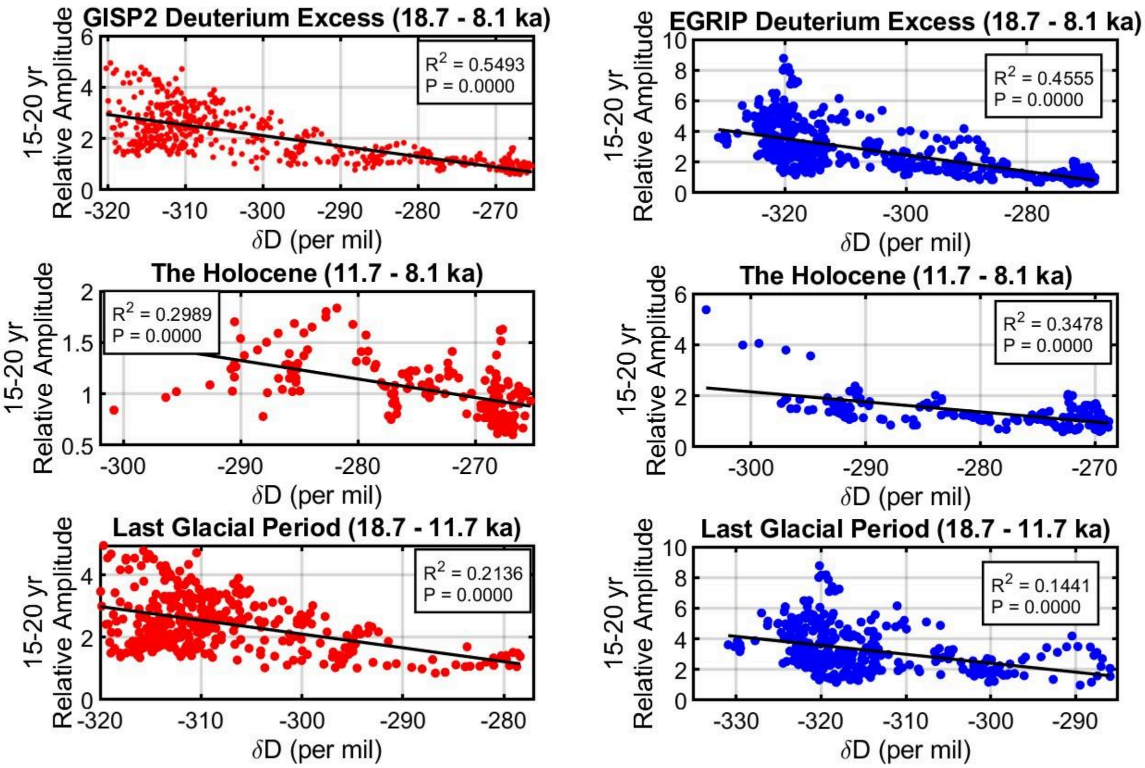

Figure 3.8: Plot of relative variability for deuterium excess value over a 15-20 yr frequency versus the mean δD isotope value (‰) over the respective window (200 yr window, 20 yr timestep). All plots contain an R^2 value and p-value that were calculated using linear regressions for the data. **(Top left)** EGRIP data from 38.5-0 ka. **(Top right)** GISP2 data from 18.7-8.1 ka. **(Middle left)** EGRIP data from 11.7-0 ka during the Holocene. **(Middle right)** GISP2 data from 11.7-8.1 ka during the Holocene. **(Bottom left)** EGRIP data from 38.5-11.7 ka during the LGP. **(Bottom right)** GISP2 data from 18.7-11.7 ka, during the LGP.

4. Discussion

Since the Holocene and Last Glacial Period (LGP) contain different climatic boundary conditions (solar insolation, greenhouse gas concentrations, ice sheet height and extent, etc.), the relationship between decadal climate variability and mean temperature, as expressed in water isotopes, can be compared to better understand the Earth climate system. The different geographies of GISP2 and EGRIP, and potentially different climatologies related to those locations, can also be compared to provide insight into differing influences on decadal variability between the two ice cores. In the following sections, I will discuss the results in the context of my hypothesis as well as the potentially broader implications of my results. I will also discuss whether these results agree with previous studies on past climate variability compared to the mean.

4.1 Comparison of Variability of Cores

The two ice cores were compared to look for differences in the decadal variability as the different geographical locations may be impacted differently. GISP2 is located near the summit of the Greenland Ice Sheet, whereas EGRIP is located on the flank of the Greenland Ice Sheet. Comparing the decadal variability in the two ice core records will test the null hypothesis that both Greenland ice cores will exhibit the same pattern of variability through time despite their geographical influences.

To further explore this relationship the records were compared in a few different ways. First, the relative amplitudes of 15-20 year variability of the two records were compared. Then, the GISP2 decadal variability record was divided by that of EGRIP. When the two records contain the same magnitude of decadal variability, then the value on the plot will be 1. If the plotted value is greater than 1, then the GISP2 decadal variability is larger than that of EGRIP at that point in the record. If the value is smaller than 1, then the opposite is true and the EGRIP decadal variability is larger at that point in the record. Lastly, the variability of the two records was plotted against each other as a scatter plot to observe the R^2 value, where a higher R^2 value correlates to a stronger relationship between the variability of the two records. Note that only high-frequency data of GISP2 from about 8.1-18.7 ka is currently available due to the ongoing reanalysis of the water isotope record. Therefore, when comparing the variability in the water isotopes between the two ice cores, only this time period is used.

4.1.1 Comparing the GISP2 and EGRIP δD Record

The raw δD isotope record of GISP2 (Figure 4.1, top left) contains similar signatures as the EGRIP δD isotope record (Figure 4.1, top right). The cold glacial period is observed from 18.7 ka until 11.7 ka when the warming climate marks the start of the Holocene. The two records, as expected, have the same general centennial and millennial scale patterns, as do all other Greenland ice cores, although there are slight differences in the magnitudes of given events, i.e. D-O Event warming, but this was not the focus of this study.

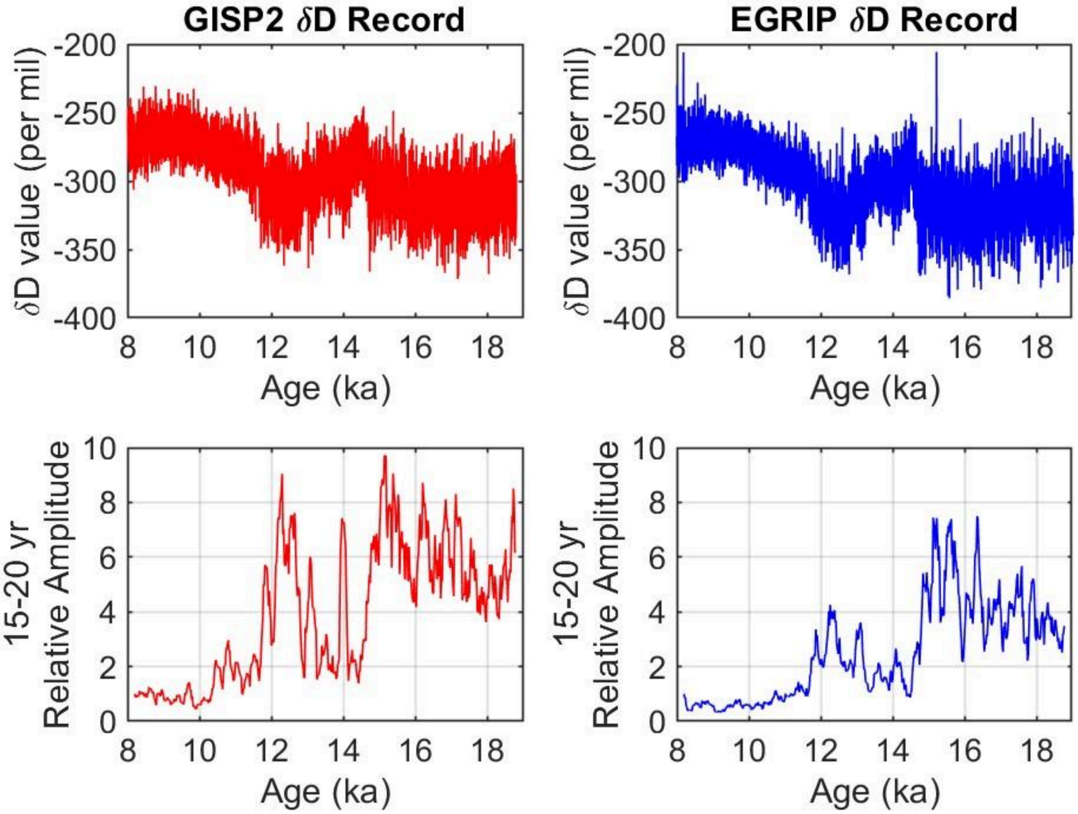

Figure 4.1: Plots of GISP2 and EGRIP δD isotope data and decadal amplitudes. **(Top left)** δD (‰) vs. Age (ka) for GISP2. **(Top right)** δD (‰) vs. Age (ka) for EGRIP. **(Bottom left)** GISP2 relative amplitudes for δD variability (relative to the 8.1-8.3 ka window, which has a value of 1) vs. Age (ka) calculated for 200 yr window size and 20 yr timestep, where average amplitudes are calculated from the average power density value within the 15-20 yr frequencies for each respective window of data and all amplitudes were then divided by the amplitude of the first window of data (8.1-8.3 ka). (**Bottom right)** EGRIP relative amplitudes vs. Age (ka), calculated with the same parameters as used for GISP2 calculations.

The relative amplitudes for both GISP2 and EGRIP (Figure 4.1 bottom figures) show three distinct variability trends throughout the record: (1) larger variability during the glacial period (18.7-14.7 ka), (2) distinct change in variability during the BA (14.7-12.9 ka) and the YD (12.9-11.7 ka), and (3) smaller, near constant, variability at the beginning of the Holocene (11.7-8.1 ka). Yet there are some notable differences in the magnitude of variability: (1) During the middle of the LGP, 18.7-14.7 ka, the relative amplitudes for GISP2 are 4-10x (with 'x' meaning x times larger than the value in the 8.1 to 8.3 ka window) and for EGRIP are 2-8x. (2) During the period 14.7-11.7 ka, both records contain overall decreased variability from 14.7-12.9 ka which is followed by a rise in variability from 12.9-11.7 ka. Although the signatures of variability are similar between the two records, GISP2 contains relative amplitudes ranging from 1.5-9x which contrasts with the relative variability of EGRIP during this period which only ranges from 1-4x. This means GISP2 contains over double the amount of relative variability at some points during this time period. This shows significant differences between the relative variability of the two records. It is also interesting to note that the relative variability of GISP2 during this time period reaches amplitudes as larger or larger than those during the LGP. The same cannot be said for the relative amplitudes of EGRIP during this period, as they almost do not reach the minimum relative amplitudes of EGRIP during the LGP. (3) During the Holocene, 11.7-8.1 ka, both records have relative amplitudes fluctuating close to 1x. From about 11.7-9.4 ka in the GISP2 record, the relative amplitudes are slightly larger than during the rest of the Holocene, as they range from 1-3x. This does not appear in the relative amplitudes of EGRIP.

The GISP2 decadal variability record was divided by the EGRIP as shown in Figure 4.2 Bottom. During the middle of the LGP, 18.7-15 ka, EGRIP's decadal variability is generally larger than that of GISP2. This is observed as the relative amplitude is consistently below 1 during this time period with GISP2's variability oscillating between being the same to half as large as that of EGRIP. This could be an effect of the climate influencing the two locations slightly differently. For 15-8.1 ka, the overall differences in the amplitudes of the records are somewhat random, ranging from GISP2 containing anywhere from half as much variability to twice as much variability compared to EGRIP. These differences may be a result of differences in how climate is expressed at the summit (GISP2) versus the flank (EGRIP).

Over many thousands of years, the signatures of higher variability in the glacial period and less variability in the Holocene support the hypothesis that the two records contain the same variability. Over shorter time scales, i.e. centennial, the decadal variability contains substantial differences where GISP2 variability can range from less than half to more than twice as large as that of EGRIP. This phenomenon where climate records agree on multi-thousand year time scales but not on smaller centennial time scales is observed in other climate records (Johnsen et al., 2001), but much more research is necessary to better understand why this occurs. Further comparison for the full GISP2 and EGRIP records is recommended for a future study to help document more situations of differences in signals.

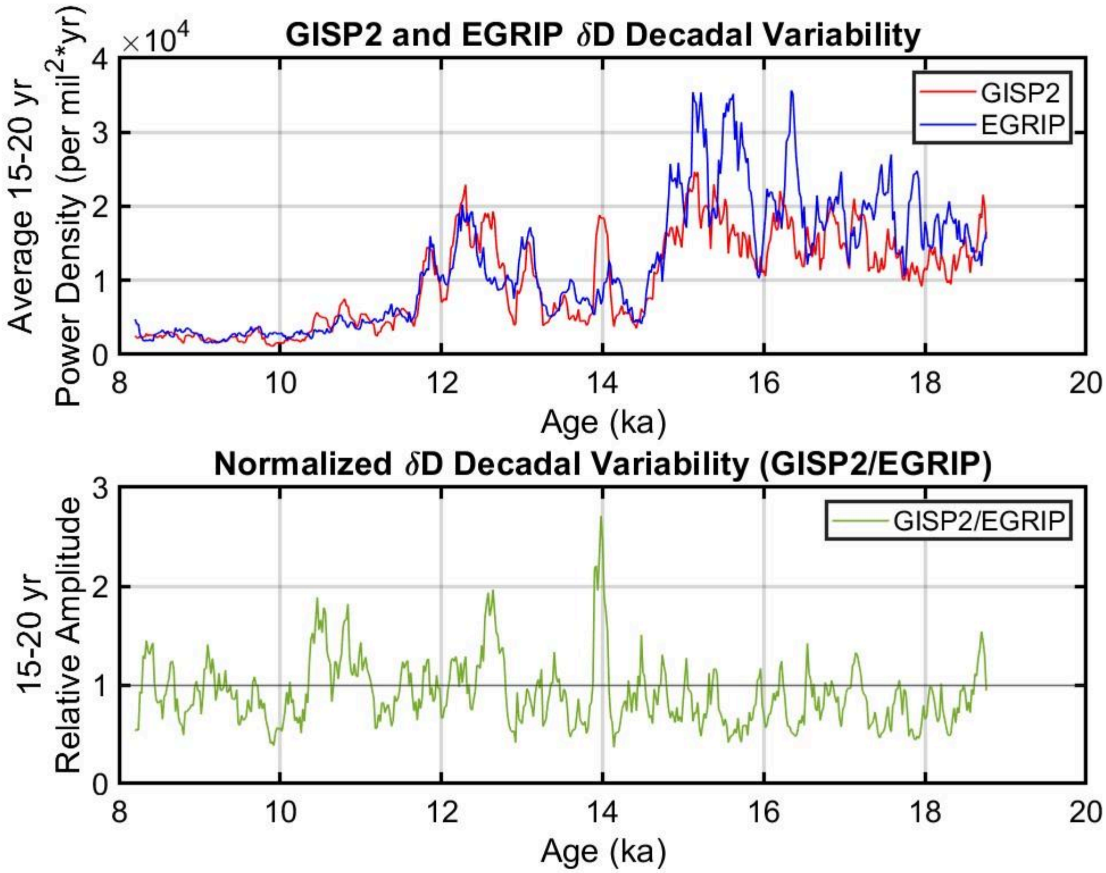

Figure 4.2: Plots comparing GISP2 and EGRIP δD isotope record amplitudes over 15-20 yr frequencies (200 yr window, 20 yr timestep). **(Top)** Average 15-20 year power density (‰^{2}yr) vs. Age (ka) of both records on the same plot. **(Bottom)** GISP2 amplitude record divided by EGRIP isotope record. Values greater than 1 are time periods when GISP2 variability was larger than EGRIP.

A scatter plot comparing the similarities in the decadal δD variability of GISP2 and EGRIP is shown in Figure 4.3. If the records are the same then the perfect linear relationship would produce an R^2 value of 1. The R^2 value of this figure is 0.6844, which means there is a somewhat strong relationship between the independent and dependent variables. The p-value of 0.000 supports a statistical relationship between the two records. This relationship is statistically significant since the p-value is 0.0000. This does not necessarily mean that the ice cores experience the same magnitude of variability and it is possible that even with a high R^2 value one record always contains higher decadal variability than the other.

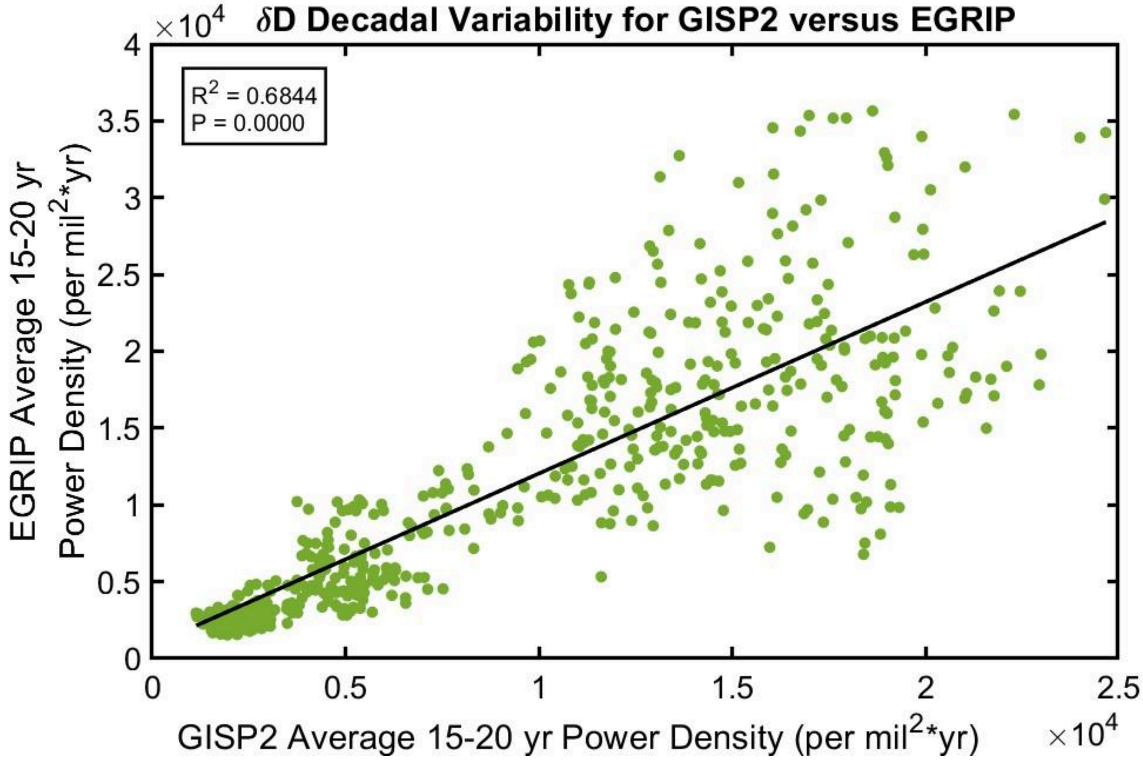

Figure 4.3: Scatter plot of power density (‰^{2}yr) for EGRIP δD decadal variability versus GISP2 δD decadal variability. The R^2 and p-value are calculated using linear regressions in MATLAB.

The above results both support and contradict my Hypothesis #2 which states, "The two ice cores are influenced by differing climatic events and will therefore contain different patterns of decadal variability in the δD and the dxs records." I found two results: 1) In support of my hypothesis, significant differences between GISP2 and EGRIP decadal variability exist on time scales of centuries. 2) My hypothesis fails on longer time scales of millennia since the variability signatures are similar. Lastly, the R^2 value (0.6544) from the scatter plot contradicts the hypothesis because it shows that the two records have some correlation between their decadal variability.

4.1.2 Comparison of GISP2 and EGRIP Deuterium Excess Variability

Throughout the record, the relative amplitudes of the dxs decadal variability show similar trends to those in the δD decadal variability plots (Figure 4.4). During the LGP (18.7-11.7 ka), the dxs relative amplitudes for GISP2 range from 1-5x (with 'x' meaning x times larger than the value in the 8.1 to 8.3 window) and 1-9x in EGRIP. Throughout the LGP, both records contain abrupt and large changes in variability. A decrease in variability occurs around 14.5-12.9 ka where variability ranges from 1-3x for GISP2 and 1-4x for EGRIP. Following this is a period of elevated dxs decadal variability. From 12.9-11.7 ka, the relative variability in GISP2 fluctuates between 1-5x and the relative variability fluctuates from 2-6x in EGRIP. The remaining part of the record (11.7-8.1 ka) is during the Holocene, which contains low, stable variability fluctuating mostly between 0.5-2x in both records. The variability is often higher in EGRIP than GISP2.

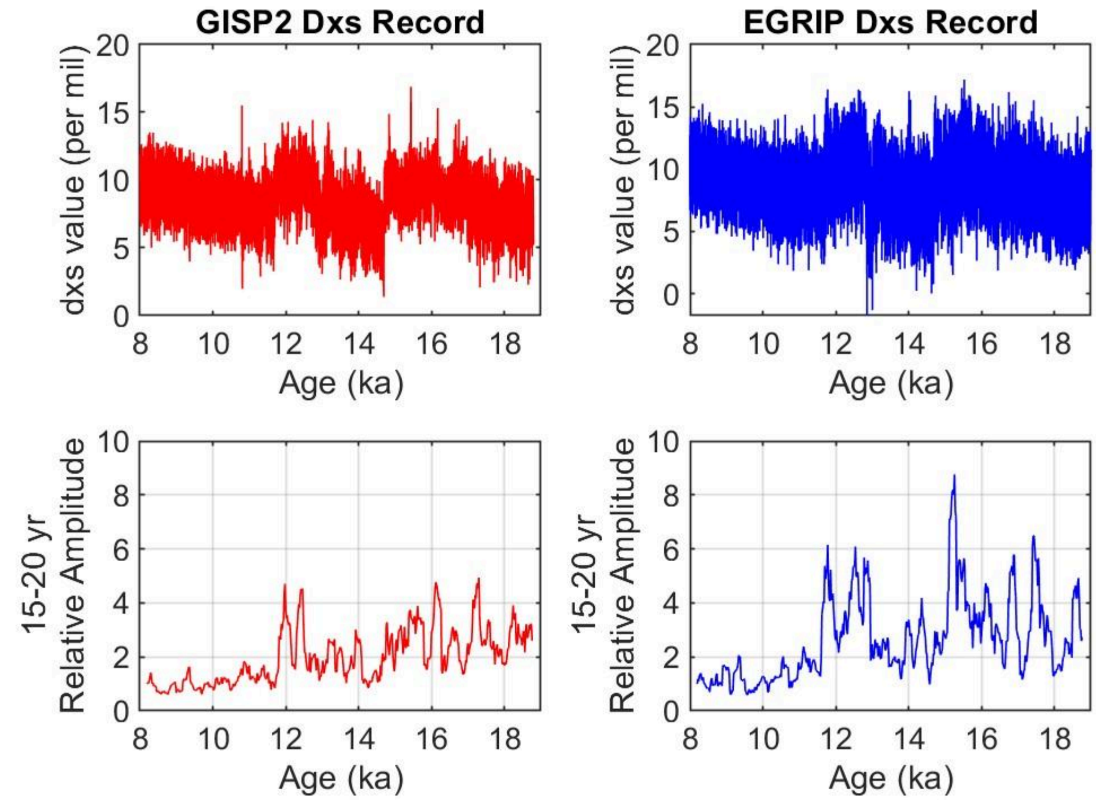

Figure 4.4: Plots of GISP2 and EGRIP deuterium excess data and high frequency amplitudes. (**Top left)** Dxs (‰) vs. Age (ka) of GISP2. (**Top right)** Dxs (‰) vs. Age (ka) of EGRIP. **(Bottom left)** GISP2 relative amplitudes for dxs variability vs. Age (ka) calculated for 200 yr window size and 20 yr timestep, where relative amplitudes are calculated from the average power density value within the 15-20 yr frequencies for each respective window of data and all amplitudes were then divided by the amplitude of the first window of data (8.1-8.3 ka). (**Bottom right)** EGRIP relative amplitudes (relative to the 8.1-8.3 ka window, which has a value of 1) for dxs variability vs. Age (ka) with window, timestep and amplitudes calculated the same as done for GISP2 plot.

It is interesting that while the variability signatures between the two records are similar (higher variability versus lower variability occurring around the same time periods), there are some potential phase offsets. For example, an increase in dxs decadal variability in EGRIP occurs at ~13 ka which is about 400 years prior to the increased variability in GISP2 (at ~12.6 ka). Another delay in variability change is observed at the end of the YD, where the variability in EGRIP decreases about 200 years after the variability in GISP2 has already decreased. This delay could be from differences in the age scale used for EGRIP and GISP2. Assuming the age scales are accurate, then the phase offsets could be a result of differences in moisture origin sources or due to sublimation differences on the ice sheet surface.

To quantify the differences in decadal dxs variability between the two records, the variability in GISP2 was divided by that of EGRIP (Figure 4.5 Bottom). Overall, this record fluctuates greatly, sometimes GISP2 dxs decadal variability is larger (values greater than 1 on the plot) and other times EGRIP is larger (values less than 1 on the plot). At two points in the record, 18.2 ka and 17.5 ka, GISP2 has over 2x the amount of variability as EGRIP. In contrast, many points exist where GISP2 variability is more than half (0.5x or less) of the decadal variability of EGRIP. The large differences between the two ice cores may be a result of differences in climatic conditions between the two ice cores or due to general noise in the climate system. Future research to understand why these climate records do not agree on centennial scales should be done along with climate modeling to investigate how the variability in dxs values are affected by geographical locations.

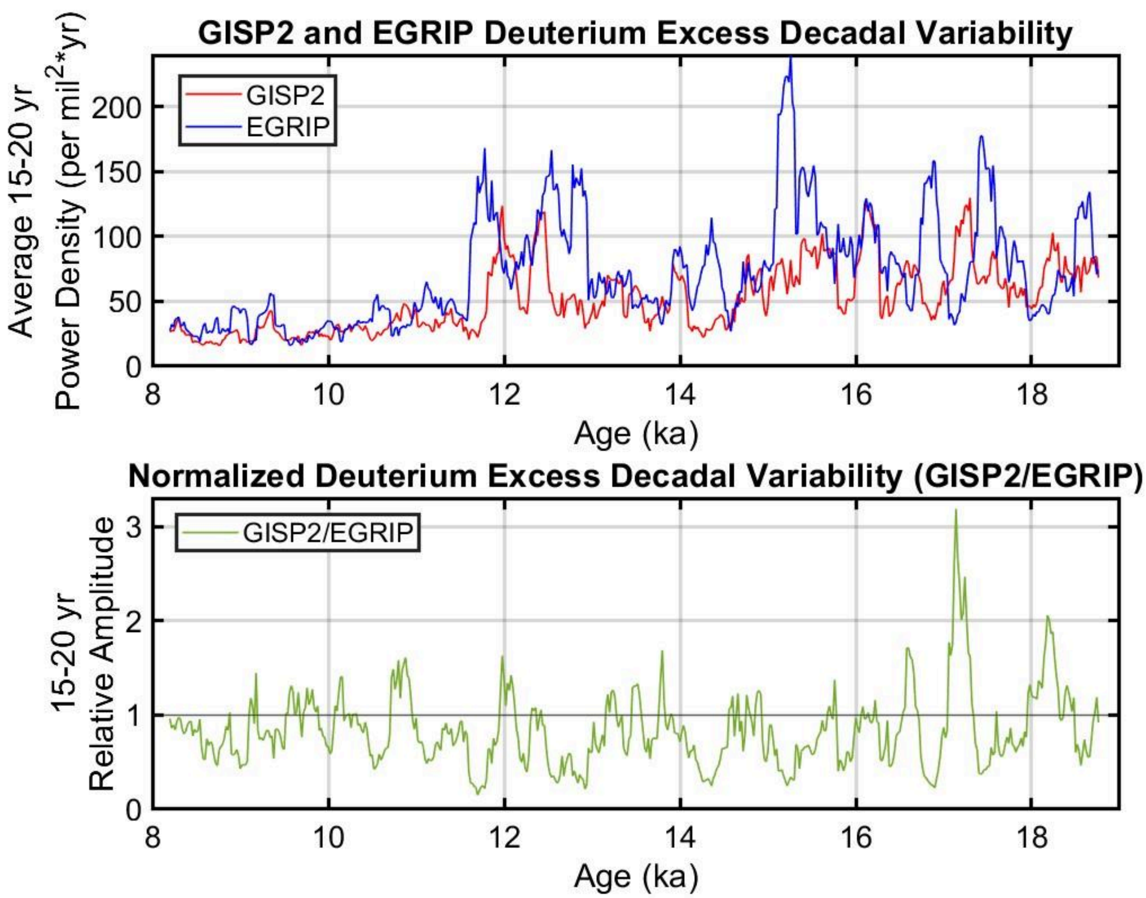

Figure 4.5: Plots comparing GISP2 and EGRIP dxs isotope record amplitudes over 15-20 yr frequencies (200 yr window, 20 yr timestep). **(Top)** Average 15-20 year power density (‰^{2}yr) vs. Age (ka) of both records on the same plot. **(Bottom)** GISP2 amplitude record divided by EGRIP

isotope record. Values greater than 1 are time periods when GISP2 variability was larger than EGRIP.

A fourth method used to compare the two records utilizes a scatter plot containing the decadal variability of dxs for GISP2 vs. EGRIP, as shown in Figure 4.6. If the records have similar influences, then changes in one record would correlate to changes in the other record which would be indicated by a higher R^2 value (closer to 1). The p-value of 0.000 means that some correlation between the two records exists but it is likely minimal. The R^2 value of 0.2403 shows a lack of a significant relationship between the dxs decadal variability of the two records.

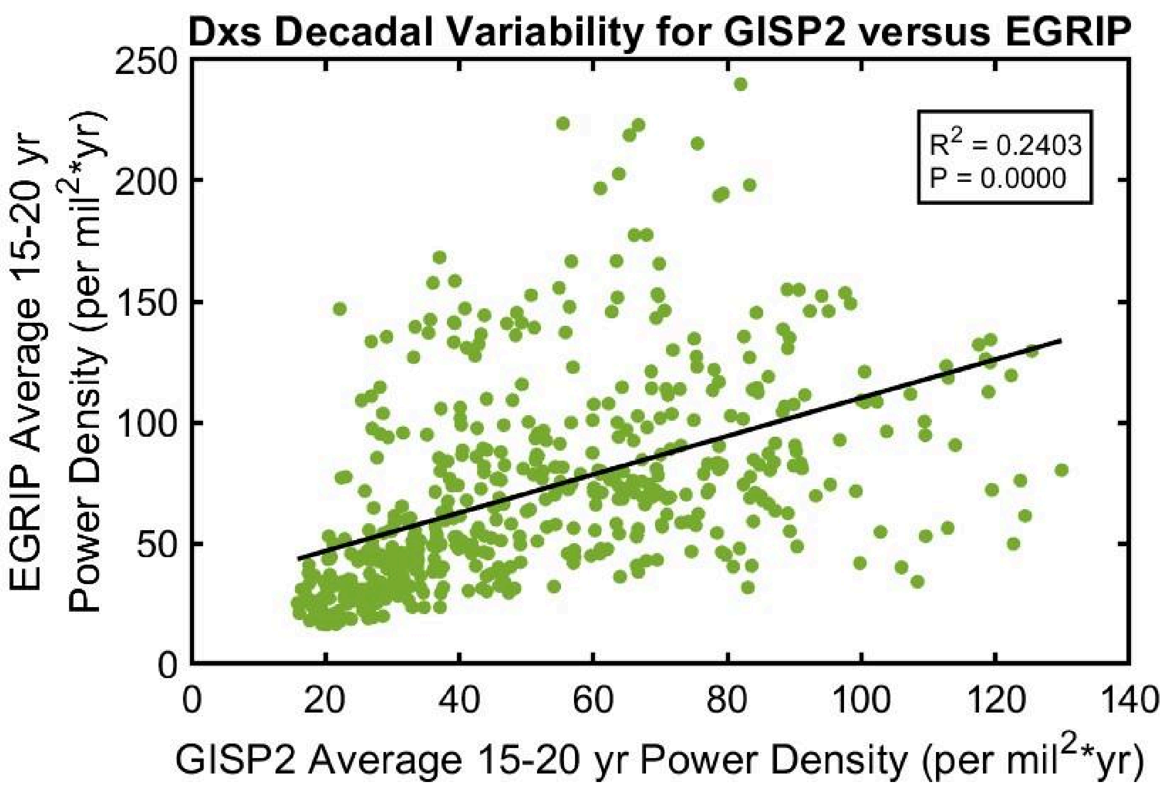

Figure 4.6: Scatter plot of GISP2 dxs decadal variability versus EGRIP dxs decadal variability. Variability is plotted as the average 15-20 year power density (‰^{2}yr). The R^2 and p-value are calculated using linear regressions in MATLAB.

The above results mainly support Hypothesis #2 in reference to dxs, which states, "The two ice cores are influenced by differing climatic events and will therefore contain different patterns of decadal variability in the δD and the dxs records." Overall the two records contain significant differences, including phase offsets for changes in variability. On average EGRIP contains larger dxs decadal variability, and a low R^2 value (0.2403) supports the hypothesis of differing climatic influences on the two ice core records. Over many thousands of years, the hypothesis fails as the records contain similar signatures of variability with higher variability during the LGP (18.7-11.7 ka) and lower variability during the Holocene (11.7-8.1 ka). This indicates that broader climatic influences exist over longer time scales, that is, across glacial-interglacial cycles, which impact the two ice core records similarly.

4.2 Does Decadal Variability in Isotopes Correlate with Temperature?

Understanding the relationship between mean temperature and decadal variability can help to understand climate drivers and what causes changes to temperature and variability. The figures explained in Results section 3.5 will be used in the following section to discuss how fluctuations in North Atlantic sea ice are likely the driver of higher variability in isotope values during colder mean temperatures (mean temperature is expressed as the average δD value over the 200 year window being observed). These figures relate variability in the isotope values to temperature and utilize linear regressions to explain how well the linear model fits the data (R^2 value) or if no statistical relationship exists (P-value below 0.05). The hypothesis tested failed since less decadal variability in isotope values occurs at higher temperatures (larger δD values).

4.2.1 Does Decadal δD Variability Correlate with Temperature?

Overall the scatter plots (Results, Figure 3.7) show two general trends where colder climates (lower δD values over 200 year averages) tend to have (1) higher δD decadal variability and (2) more variability of the δD decadal variability, that is, more scatter in the data points for δD decadal variability exists in the glacial climate than the Holocene.

First, I will discuss point #1. This result is interesting because one might generally think that with warmer temperatures, more energy in the climate system would translate into higher δD decadal variability. But of course, the climate system is not so simple, and my results show the opposite. When observing the entire available GISP2 record, an R^2 value of 0.6844 shows an inverse relationship between mean temperature and δD decadal variability. Fluctuations in sea ice are a proposed driver of δD decadal variability during the LGP (Brashear et al., 2025). It is possible that greater north-south fluctuations in the sea-ice edge during colder, stadial periods are the cause of the inverse relationship with mean temperature. My results provide evidence in support of previous findings which suggest fluctuations in North Atlantic sea ice affect δD decadal variability, but further research and modeling are necessary as more of the high-resolution GISP2 water isotope record is available.

Pertaining to my second point above, with warmer mean temperatures, the δD decadal variability data points fluctuate over a smaller range. For example, in GISP2 Figure 3.7, for a mean δD of about -270‰, the δD decadal variability data points that correspond to those mean δD values fluctuate between 0.5-1x. However, contrast this with mean δD of about -310‰, where δD decadal variability data points fluctuate between 3-9x. Similar results occur for the EGRIP scatter plots. The larger spread in δD decadal variability with colder mean temperatures may also be a result of fluctuations in North Atlantic sea ice.

The above results do not support my original Hypothesis #1, which states "As mean temperature increases, the decadal variability in the δD and the dxs values will also increase." I find the opposite, as mean temperature increases, the decadal variability in the δD decreases. I discuss the dxs part of this hypothesis below.

4.2.2 Does Decadal Dxs Variability Correlate with Temperature?

Deuterium excess (dxs) is mainly influenced by a few variables, including the conditions at the moisture origin point (sea surface temperature, humidity of the air above the sea, and winds above the sea surface), but also sublimation at the ice sheet surface. Therefore decadal variability in dxs will relate to these variables. Similar results to δD are observed for decadal variability in dxs (Results, Figure 3.8): (1) larger decadal variability in dxs occurs with colder temperatures and (2) more variability of the dxs decadal variability occurs at lower temperatures, that is, more scatter in the data points for dxs decadal variability exists in the glacial climate than the Holocene.

First I will discuss the first point above, about observing increased variability in dxs with decreasing mean temperatures. The entire GISP2 record contains an R^2 value of 0.5493 and p-value of 0.000, showing an inverse relationship between the dxs variability and mean temperatures. The dxs variability may also be a result of greater fluctuations in North Atlantic sea ice during the LGP than exist today. If more north-south movement of the sea-ice edge occurs with colder stadial periods, this likely also results in more variability in the moisture origin conditions fluctuating. For example, if a large decadal-scale shift in the sea ice edge occurs shifting the ice edge very far south, then the moisture source (or the combination of sources) also must shift south, and the relative humidity and temperature of the sea surface will almost certainly change. This explanation provides further evidence in favor of fluctuations in the North Atlantic sea ice edge driving decadal variability in water isotope values (in this case for dxs) which is the same as mechanisms proposed by Brashear et al. (2025) for δD decadal variability changes.

The second point above, mentions the observation of a larger spread of decadal variability in dxs during colder climates compared to warmer climates. During colder climates, the dxs variability can range up to 5 times more than during the warmer climates (i.e. variability ranging from 1.5-5x at -315‰ compared to 0.5-1.7x at -270‰). Similar results are observed for EGRIP where the range of variability increases with decreasing mean temperatures. The increased range of variability may also be a result of fluctuations in North Atlantic sea ice, but further modeling would be necessary for more conclusive results.

The results for decadal variability in dxs do not support my original Hypothesis #1, which states "As mean temperature increases, the decadal variability in the δD and the dxs values will also increase." I instead found that as mean temperature increases, the decadal variability in the dxs decreases. Observations in dxs variability in this thesis are preliminary results. Future studies should further document and model decadal variability in dxs, including replicating this analysis with the entire high-resolution GISP2 record once it is available.

4.3 Does Decadal Variability Change at the Same Time as Abrupt Warming Events?

The relationship between mean temperature (200 year averages) and decadal variability in temperature can provide insight into climatic drivers. Brashear et al. (2025) observed a phase offset in which variability changes a few hundred years before an abrupt warming event (D-O Event) occurs. It is important that this phase offset is documented in other ice cores to show its reproducibility and validity. One of the major goals of resampling GISP2 is to create another high-resolution record where this phase offset can be observed.

In this thesis, I checked for phase offsets for two abrupt warming events that occur in the available section of the high-resolution GISP2 water isotope record: (1) the Bolling-Allerod (BA) and (2) the end of the Younger Dryas (YD), which marks the start of the Holocene, as shown in Figure 4.7. Both records show two separate decreases in variability relative to the start of the abrupt increase in temperature. The warming of the BA begins at about 14.75 ka when δD values begin to increase. An initial decrease in variability occurs at ~15.2 ka until ~15 ka followed by another decrease in variability beginning about 14.75 ka, coinciding with the onset of the abrupt warming at the start of the BA. Essentially the decrease in variability seems to occur in multiple steps. A similar signature occurs at the end of the YD. Many hundreds of years prior to the abrupt warming, which begins at ~11.7 ka, an initial decrease in variability occurs at ~12.3 ka. After this initial decrease in variability, an increase in variability occurs for a few hundred years, followed by another decrease in variability that seems to align with the abrupt warming at the end of the YD.

Based on available results, Hypothesis #3 stating, “No phase offset exists between changes in decadal variability compared to abrupt warming of D-O Events in GISP2,” is inconclusive. Both cases I tested (BA and end of YD) show two decreases in variability, one that occurs hundreds of years before the onset of the abrupt warming event and another that is concurrent with abrupt warming. But it is difficult to separate between the noisiness of the climate system and a true regime shift in decadal variability. That is, it is not clear how to determine when decadal variability begins to decline, in the first case decreasing variability leads to abrupt warming by hundreds of years (as in Brashear et al., 2025), and in the second case, there is no phase offset. As more D-O Events are analyzed in the GISP2 record (as will occur after the submission of this thesis), a clearer understanding of any phase offset will emerge.

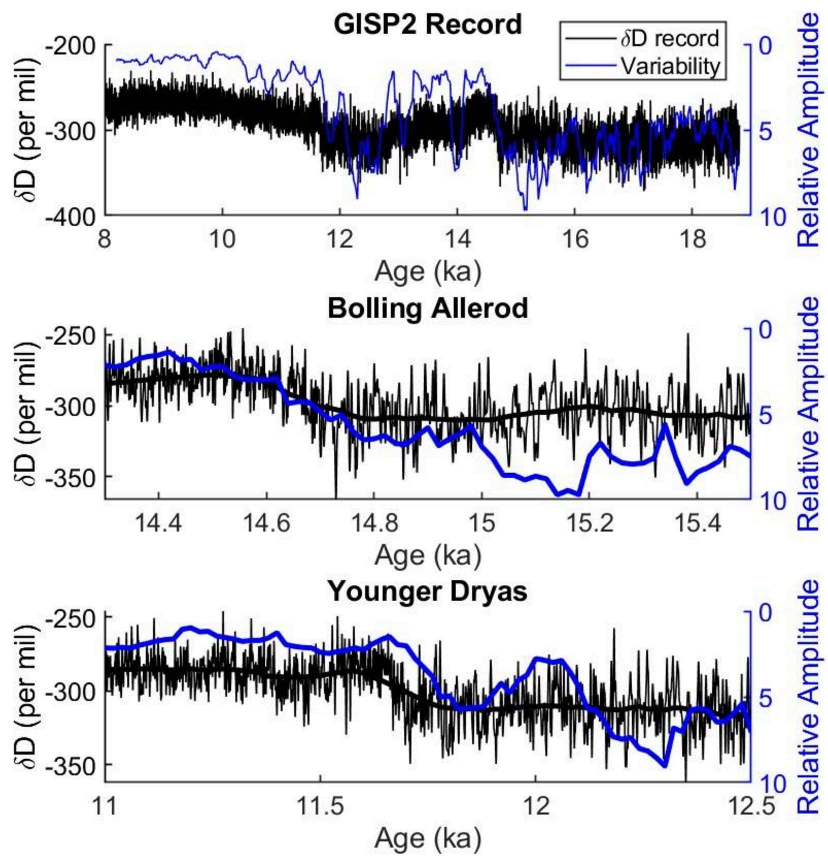

Figure 4.7: Plots of GISP2 δD (‰) on y-axis 1 (left y-axis) vs Age (ka) and relative amplitudes (note the variability scale is reversed so larger variability is lower and less variability is at the top; amplitudes over 15 to 20 yr frequency; 200 yr window; 20 yr time step) on y-axis 2 (right y-axis) vs Age (ka). **(Top)** Entire available GISP2 δD record. **(Middle)** Zoomed in section from 15.5-13.5 ka over the BA event. **(Bottom)** Zoomed in section from 13.5-11 ka during the end of YD and the start of Holocene.

4.4 Uncertainty

There are a number of potential sources of uncertainty that I have not fully accounted for in the results of this thesis. Two of those sources are beyond the scope of the project, but I mention them below for completeness. A third source has to do with replicating results across different frequency bands, which I also include below.

4.4.1 Randomness of the Climate System

Sometimes what is actually randomness in climate data can appear to have a trend. To illustrate this point, white noise plots can be generated that have the same mean and standard deviation as the actual ice core data we are interested in. Figure 4.8 shows a plot of white noise that was generated using parameters of the EGRIP δD isotope record. The white noise data was then analyzed to determine the decadal variability, in the same way as done for prior plots such as Figure 3.3 and 3.5. Throughout the entire simulated record the relative amplitudes of the decadal variability mostly fluctuate between 0.5 and 2. While not an exhaustive exercise, this demonstrates that with white noise generated using the same parameters as that of actual ice core data, decadal variability can vary by as much as a factor of two for different time periods within the generated white noise. Similar results can be expected in the climate system, which also exhibits randomness meaning that at certain times we may see a change in decadal variability that is literally the result of random changes to the climate rather than due to some forcing mechanism like changes in sea ice.

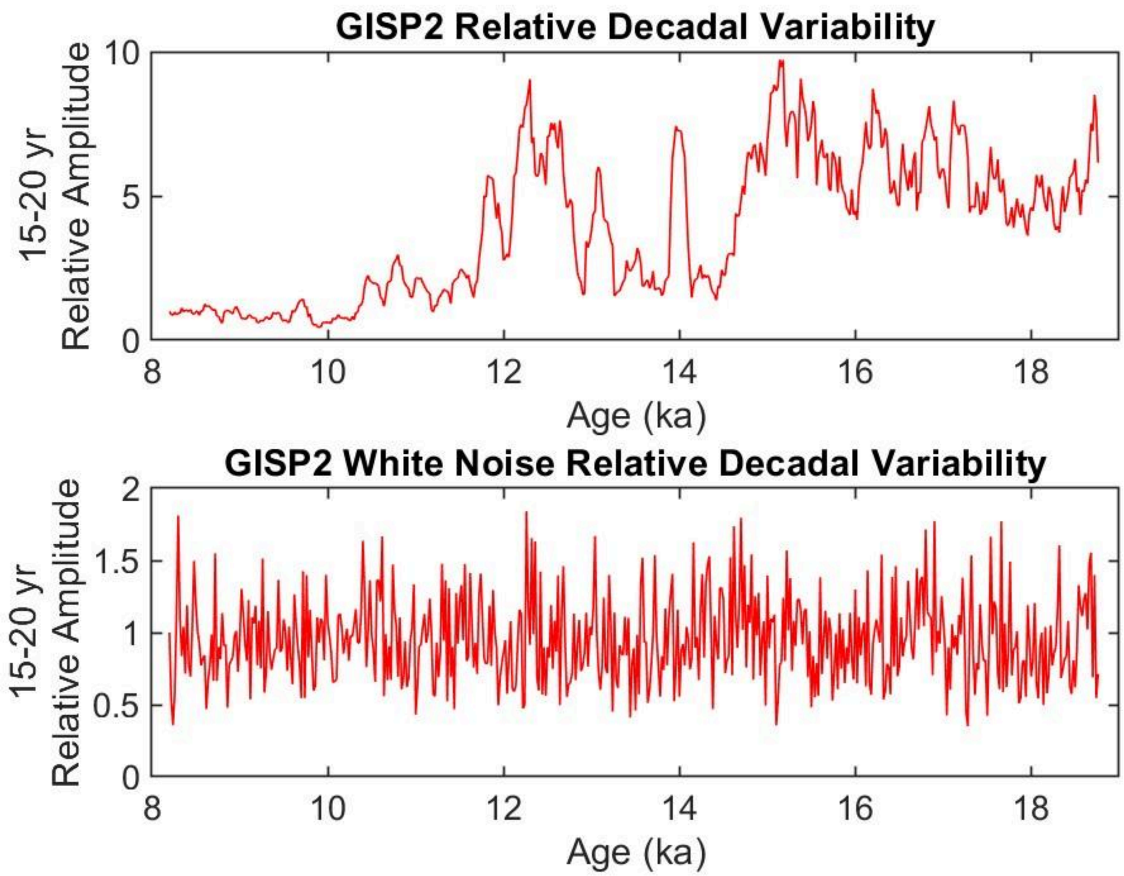

Figure 4.8: Plots of GISP2 δD relative amplitudes vs. Age (ka) for the actual record and a simulated record. **(Top)** The actual record used to calculate average amplitudes are calculated from the average power density value within the 15-20 yr frequencies for each respective window of data and all amplitudes were then divided by the amplitude of the first window of data (8.1-8.3 ka) to calculate the relative amplitudes of the record. **(Bottom)** Simulated climate variability in the form of white noise, generated using the parameters of the EGRIP δD isotope record, including mean and standard deviation of the isotope data. The white noise data was then analyzed for decadal variability (15-20 year band) with windows of 200 years and 20 year time steps.

4.4.2 Testing Reproducibility of Decadal Variability within Different Frequency Bands

Different frequency bands in ice core water isotope records may contain different patterns of variability through time. Throughout this paper, the frequency band of 15-20 years was used to interpret decadal variability. This frequency was chosen since it is minimally affected by diffusion, but any decadal frequency band, from 10-30 years, could have been chosen to fit the climate signal. Does the use of different frequency bands change the results of this thesis? The results of a sensitivity analysis for different frequency bands (10-15 yr, 15-20 yr, 20-30 yr) are shown in Figure 4.9. For the 10-15 yr band, the signal is decreased significantly from the other two bands. The 15-20 yr band has a similar signal to that of the 20-30 yr band. One reason that the 15-20 and 20-30 yr bands are elevated over the 10-15 yr band is an effect in climate data known as red noise. Red noise indicates lower and lower power density or amplitude of signals as the frequency increases. The decadal bands being interpreted here fall within this red noise zone (Huybers and Curry 2006), so we would expect the 20-30 yr band to have a larger relative amplitude than the 10-15 yr band. However, more importantly, over long time scales (many thousands of years) all bands show the same signal, which is elevated relative amplitudes in the glacial and smaller relative amplitudes in the Holocene. It was beyond the scope of the thesis to compare frequency bands over shorter time scales such as for D-O Events, but this would be an interesting exercise to determine if relative amplitudes across frequency bands behave the same way for abrupt warming events

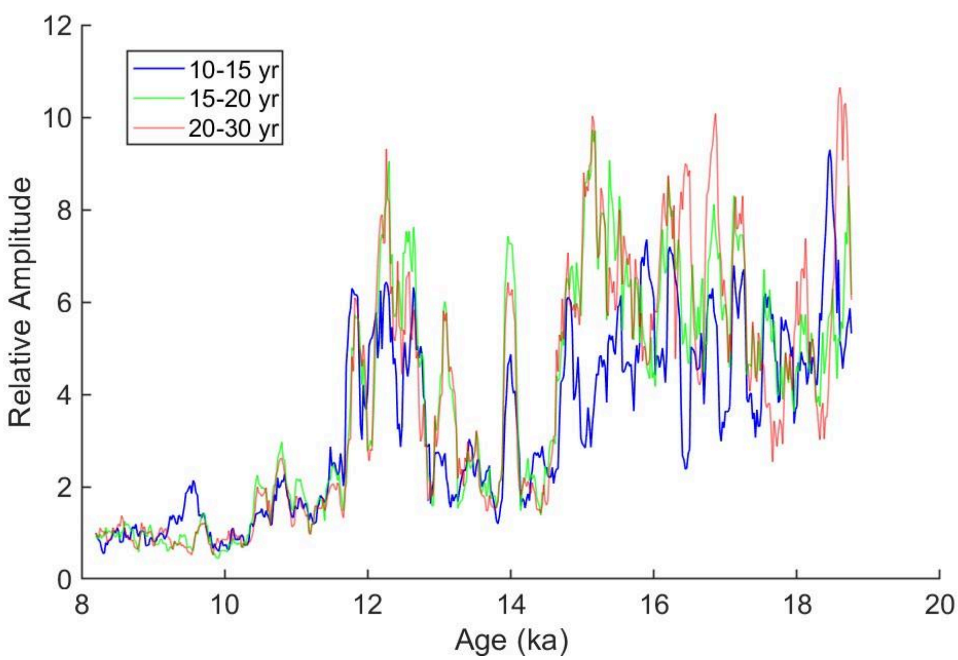

Figure 4.9: Relative amplitudes of GISP2 δD isotope record over various frequency bands versus age (ka). 10-15 yr frequency in blue, 15-20 yr in green, and 20-30 yr in red. (200 yr window, 20 yr timestep)

4.4.3 Diffusion

Diffusion is a known effect that can alter water isotope records within an ice sheet. The top ~50-100 m of an ice sheet is a styrofoam-like layer where the snow is compressing into ice, known as the firn layer. In this layer many air pathways exist in which water molecules tend to spread out within the air pathways due to diffusion (Grew and Ibbs, 1952; Johnsen, 1977; Whillans and Grootes, 1985). Diffusion decreases the amplitude of the highest frequencies of an ice core water isotope record. It will even eliminate some high-frequency signals entirely. Such is the case for Greenland ice cores, which rarely contain annual signals since they have been diffused away in the firn. In high-frequency isotope records, like GISP2 and EGRIP, decadal time scales do not need to be corrected for diffusion since the records retain the decadal scale variability signatures, that is, diffusion hardly decreases the amplitude of decadal signals. This is shown in Brashear et al. (2025), where a diffusion correction for the EGRIP δD isotope record is performed. Figure 4.10 shows a diffusion-corrected power density plot for a 400 yr window of time from Brashear et al. (2025). The period analyzed in this thesis is over the 15-20 yr frequency band, highlighted in blue in the figure, and does not need to be corrected. Diffusion only affects the amplitudes of frequencies above 10 years when the black line bends downwards which is the telltale sign of diffusion in water isotope records. EGRIP has a lower accumulation rate than GISP2, so, the effects of diffusion will be even less for the GISP2 ice core. With more accumulation, water molecules have to travel further to pass the boundaries of annual layers of snow during the diffusion process, thus with more accumulation there is less diffusion.

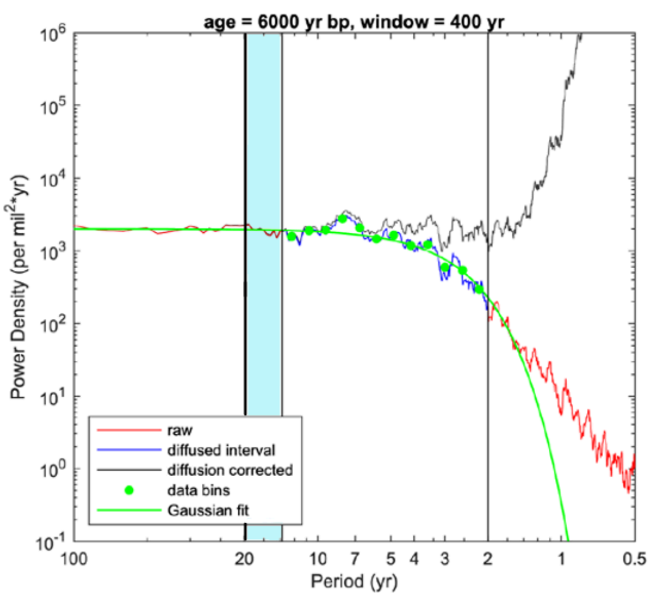

Figure 4.10: Diffusion corrected plot of power density (per mil^2*yr) vs. period (yr) from Brashear et al. (2025). Plot for 400 yr window of time from 6000 ka. The highlighted blue section (15-20 yr period) shows the frequency used for analysis.

5. Conclusion

Using spectral analysis of two high-resolution ice cores from Greenland, GISP2 and EGRIP, I observed how the water isotope variability over the 15-20 year frequency band changes through the records (from 8.1-18.7 ka) and compared the variability change in the records to each other and to average temperature over windows of 200 years. GISP2 is an ongoing resampling project from the archives of an ice core originally drilled in the early 1990s. As of the time of this thesis, only a portion of the record was available for analysis, but when the entire record is available these analyses should be again performed for the entire record, as it will date back to about 100 ka or older. The entire GISP2 record will also provide the opportunity for a more comprehensive comparison of climatic signatures between the two ice cores.

Overall many of my results agree with prior findings, including increased decadal variability in water isotopes with colder climates. The drivers of increased variability with colder climates should be further studied for better understanding, but for now, my findings support fluctuations in sea ice being a large governing factor of decadal climate variability, as shown in Brashear et al. (2025). When comparing the two ice cores, my results suggest that decadal-scale climate is expressed differently between the two locations on centennial time scales but contains similar signatures on millennial time scales. Additionally, the decadal variability in dxs between the two ice cores was significantly different, as indicated by a low R^2 value (0.2403). In contrast, the decadal variability in δD between the two ice cores contains a higher R^2 value (0.6844), suggesting a stronger relationship. Lastly, the relationship between decadal δD decadal variability and abrupt warming events (D-O Events) for GISP2 did not fully agree with prior findings for EGRIP in that I could not definitively find a lead-lag relationship between decadal δD variability and mean temperature (Brashear et al. 2025).

My recommendation is that every future ice core is done at high resolution so that we can continue to utilize variability's relation to mean temperature or moisture origin source (sea surface) conditions to understand climate drivers over different time scales. Future studies should also confirm whether a lead-lag relationship exists for other D-O Events recorded in the GISP2 record to look for further agreement with Brashear et al. (2025). We also need future studies that use models that specifically observe changes in ice sheets and sea ice relative to shifts in decadal amplitudes during D-O Events to better understand drivers of changes in variability and mean temperature.

6. References

Armstrong, E., Izumi, K., & Valdes, P. (2022). Identifying the mechanisms of DO-scale oscillations in a GCM: A salt oscillator triggered by the Laurentide ice sheet. *Climate Dynamics*, *60*, 1–19. https://doi.org/10.1007/s00382-022-06564-y

Arthur, M. A., & Garrison, R. E. (1986). Cyclicity in the Milankovitch band through geologic time: An introduction. *Paleoceanography, 1*(4), 369–372. https://doi.org/10.1029/PA001i004p00369

Axtell, R. L., Epstein, J. M., Dean, J. S., Gumerman, G. J., Swedlund, A. C., Harburger, J., Chakravarty, S., Hammond, R., Parker, J., & Parker, M. (2002). Population growth and collapse in a multiagent model of the Kayenta Anasazi in Long House Valley. *Proceedings of the National Academy of Sciences of the United States of America, 99*(Suppl 3), 7275-7279.

Barnola, J. M., Raynaud, D., Korotkevich, Y. S., & Lorius, C. (1987). Vostok ice core provides 160,000-year record of atmospheric CO2. *Nature*, *329*(6138), 408–414. https://doi.org/10.1038/329408a0

Bernard, M. (1942). Precipitation. In O. E. Meinzer (Ed.), *Hydrology* (Chap. II). Dover.

Berner, W., Oeschger, H., & Stauffer, B. (1980). Information on the CO2 Cycle from Ice Core Studies. *Radiocarbon*, *22*(2), 227–235. https://doi.org/10.1017/S0033822200009498

Bierkens, M. F. P. (2015). Global hydrology 2015: State, trends, and directions. *Water Resources Research, 51*(7), 4923–4947. https://doi.org/10.1002/2015WR017173

Bird, M. I., Haig, J., Hadeen, X., Rivera-Araya, M., Wurster, C. M., & Zwart, C. (2020). Stable isotope proxy records in tropical terrestrial environments. *Palaeogeography, Palaeoclimatology, Palaeoecology*, *538*, 109445. https://doi.org/10.1016/j.palaeo.2019.109445

Bjerknes, J. (1969). Atmospheric teleconnections from the equatorial Pacific. *Monthly Weather Review, 97*, 163–172. https://doi.org/10.1175/1520-0493(1969)097<0163:ATFTEP>2.3.CO;2

Boers, N. (2018). Early-warning signals for Dansgaard-Oeschger events in a high-resolution ice core record. *Nature Communications, 9*(1). https://doi.org/10.1038/s41467-018-04881-7

Brashear, C. A., Jones, T. R., Morris, V., Vaughn, B. H., Roberts, W. H. G., Skorski, W. B., Hughes, A. G., Nunn, R., Rasmussen, S. O., Cuffey, K. M., Vinther, B. M., Sowers, T., Buizert, C., Gkinis, V., Holme, C., Jensen, M. F., Kjellman, S. E., Langebroek, P. M., Mekhaldi, F., … White, J. W. C. (2025). Shifts in Greenland interannual climate variability lead Dansgaard–Oeschger abrupt warming by hundreds of years. *Climate of the Past*, *21*(2), 529–546. https://doi.org/10.5194/cp-21-529-2025

Broecker, W. S., Bond, G., Klas, M., Bonani, G., & Wolfli, W. (1990). A salt oscillator in the glacial Atlantic? 1. The concept. *Paleoceanography*, *5*(4), 469–477. https://doi.org/10.1029/PA005i004p00469

Broecker, W. S. (1998). Paleocean circulation during the Last Deglaciation: A bipolar seesaw? *Paleoceanography*, *13*(2), 119–121. https://doi.org/10.1029/97PA03707

Carrillo, C. N. (1893). Boletín de la Sociedad Geográfica de Lima. *Hidrografía Oceánica, 1*, 72–110.

Chahine, M. T. (1992). The hydrological cycle and its influence on climate. *Nature, 359*(6394), 373–380. https://doi.org/10.1038/359373a0

Charles, C. D., Rind, D., Jouzel, J., Koster, R. D., & Fairbanks, R. G. (1994). Glacial-Interglacial Changes in Moisture Sources for Greenland: Influences on the Ice Core Record of Climate. *Science, 263*(5146), 508–511. https://doi.org/10.1126/science.263.5146.508

Cole-Dai, J., Ferris, D., Lanciki, A., Savarino, J., Baroni, M., & Thiemens, M. H. (2009). Cold decade (AD 1810–1819) caused by Tambora (1815) and another (1809) stratospheric volcanic eruption. *Geophysical Research Letters*, *36*(22). https://doi.org/10.1029/2009GL040882

Craig, H., & Gordon, L. J. (1965). Stable Isotopes in Oceanographic Studies. Laboratorio di Geologia Nucleare Pisa, 9-130.

Craig, H. (1961). Isotopic variations in meteoric waters. *Science, 133*, 1702-1703.

Crosson, E. R. (2008). A cavity ring-down analyzer for measuring atmospheric levels of methane, carbon dioxide, and water vapor. *Applied Physics B*, *92*(3), 403–408. https://doi.org/10.1007/s00340-008-3135-y

Cuffey, K. M., Clow, G. D., Alley, R. B., Stuiver, M., Waddington, E. D., & Saltus, R. W. (1995). Large Arctic Temperature Change at the Wisconsin-Holocene Glacial Transition. *Science, 270*(5235), 455–458. https://doi.org/10.1126/science.270.5235.455

Dansgaard, W., Johnsen, S. J., Clausen, H. B., Dahl-Jensen, D., Gundestrup, N. S., Hammer, C. U., Hvidberg, C. S., Steffensen, J. P., Sveinbjörnsdottir, A. E., Jouzel, J., & Bond, G. (1993). Evidence for general instability of past climate from a 250-kyr ice-core record. *Nature*, *364*(6434), 218–220. https://doi.org/10.1038/364218a0

Dansgaard, W. (1964). Stable isotopes in precipitation. *Tellus*, *16*(4), 436–468. https://doi.org/10.1111/j.2153-3490.1964.tb00181.x

Dee, S., Bailey, A., Conroy, J. L., Atwood, A., Stevenson, S., Nusbaumer, J., & Noone, D. (2023). Water isotopes, climate variability, and the hydrological cycle: Recent advances and new frontiers. *Environmental Research: Climate*, *2*(2), 022002. https://doi.org/10.1088/2752-5295/accbe1

Delmas, R. J. (1992). Environmental information from ice cores. *Reviews of Geophysics*, *30*(1), 1–21. https://doi.org/10.1029/91RG02725

Dokken, T. M., Nisancioglu, K. H., Li, C., Battisti, D. S., & Kissel, C. (2013). Dansgaard-Oeschger cycles: Interactions between ocean and sea ice intrinsic to the Nordic seas. *Paleoceanography*, *28*(3), 491–502. https://doi.org/10.1002/palo.20042

EPICA Community Members (2006). One-to-one coupling of glacial climate variability in Greenland and Antarctica. *Nature, 444*(7116), 195-198.

Gat, J. R. (1996). Oxygen and hydrogen isotopes in the hydrologic cycle. *Annual Review of Earth and Planetary Sciences, 24*, 225–262. https://doi.org/10.1146/annurev.earth.24.1.225

Gerber, T. A., Hvidberg, C. S., Rasmussen, S. O., Franke, S., Sinnl, G., Grinsted, A., Jansen, D., & Dahl-Jensen, D. (2021). Upstream flow effects revealed in the EastGRIP ice core using Monte Carlo inversion of a two-dimensional ice-flow model. *The Cryosphere, 15*(8), 3655–3679. https://doi.org/10.5194/tc-15-3655-2021

Ghil, M. (2002). Natural climate variability. In *Encyclopedia of Global Environmental Change* (Vol. 1, pp. 544–549). John Wiley & Sons, Ltd.

Gill, R. B. The great Maya droughts: water, life, and death. *UNM Press*, 2001.

Gkinis, V., Popp, T. J., Blunier, T., Bigler, M., Schüpbach, S., Kettner, E., & Johnsen, S. J. (2011). Water isotopic ratios from a continuously melted ice core sample. *Atmospheric Measurement Techniques*, *4*(11), 2531–2542. https://doi.org/10.5194/amt-4-2531-2011

Gkinis, V., Simonsen, S. B., Buchardt, S. L., White, J. W. C., & Vinther, B. M. (2014). NorthGRIP firn temperature reconstruction based on water isotope firn diffusion [dataset]. In *Supplement to: Gkinis, V et al. (2014): Water isotope diffusion rates from the NorthGRIP ice core for the last 16,000 years – Glaciological and paleoclimatic implications. Earth and Planetary Science Letters, 405, 132-141, https://doi.org/10.1016/j.epsl.2014.08.022*. PANGAEA. https://doi.org/10.1594/PANGAEA.871566

Gkinis, V., Vinther, B. M., Popp, T. J., Quistgaard, T., Faber, A.-K., Holme, C. T., Jensen, C.-M., Lanzky, M., Lütt, A.-M., Mandrakis, V., Ørum, N.-O., Pedersen, A.-S., Vaxevani, N., Weng, Y., Capron, E., Dahl-Jensen, D., Hörhold, M., Jones, T. R., Jouzel, J., … White, J. W. C. (2021). A 120,000-year long climate record from a NW-Greenland deep ice core at ultra-high resolution. *Scientific Data*, *8*(1), 141. https://doi.org/10.1038/s41597-021-00916-9

Gleick, P. H., Cooley, H., Famiglietti, J. S., Lettenmaier, D. P., Oki, T., Vörösmarty, C. J., & Wood, E. F. (2013). Improving Understanding of the Global Hydrologic Cycle. In G. R. Asrar & J. W. Hurrell (Eds.), *Climate Science for Serving Society: Research, Modeling and Prediction Priorities* (pp. 151–184). Springer Netherlands. https://doi.org/10.1007/978-94-007-6692-1_6

Grew, K. E., and T. L. Ibbs (1952), Thermal Diffusion in Gases, *Cambridge Univ. Press, Cambridge.*

Grootes, P. M., Stuiver, M., White, J. W. C., Johnsen, S., & Jouzel, J. (1993). Comparison of oxygen isotope records from the GISP2 and GRIP Greenland ice cores. *Nature, 366*(6455), 552–554. https://doi.org/10.1038/366552a0

Hodell, D. A., Curtis, J. H., & Brenner, M. (1995). Possible role of climate in the collapse of Classic Maya civilization. Nature, 375(6530), 391-394.

Hughes, A. G., Jones, T. R., Vinther, B. M., Gkinis, V., Stevens, C. M., Morris, V., Vaughn, B. H., Holme, C., Markle, B. R., & White, J. W. C. (2020). High-frequency climate variability in the Holocene from a coastal-dome ice core in east-central Greenland. *Climate of the Past*, *16*(4), 1369–1386. https://doi.org/10.5194/cp-16-1369-2020

Huybers, P., & Curry, W. (2006). Links between annual, Milankovitch and continuum temperature variability. *Nature, 441*(7091), 329–332. https://doi.org/10.1038/nature04745

Huybers, P. (2021). pmtmPH.m (https://www.mathworks.com/matlabcentral/fileexchange/2927-pmtmph-m), MATLAB Central File Exchange. Retrieved September 13, 2024.

Imbrie, J., Boyle, E. A., Clemens, S. C., Duffy, A., Howard, W. R., Kukla, G., Kutzbach, J., Martinson, D. G., McIntyre, A., Mix, A. C., Molfino, B., Morley, J. J., Peterson, L. C., Pisias, N. G., Prell, W. L., Raymo, M. E., Shackleton, N. J., & Toggweiler, J. R. (1992). On the Structure and Origin of Major Glaciation Cycles 1. Linear Responses to Milankovitch

Forcing. *Paleoceanography and Paleoclimatology*, 7(6), 701–738. https://doi.org/10.1029/92PA02253
Johnsen, S. J., Clausen, H. B., Dansgaard, W., Fuhrer, K., Gundestrup, N., Hammer, C. U., Iversen, P., Jouzel, J., Stauffer, B., & Steffensen, J. P. (1992). Irregular glacial interstadials recorded in a new Greenland ice core. *Nature, 359*(6393), 311–313. https://doi.org/10.1038/359311a0
Johnsen, S. J., Dahl-Jensen, D., Dansgaard,W., & and Gundestrup, N. (1995). Greenland palaeotemperatures derived from GRIP bore hole temperature and ice core isotope profiles. Tellus B: *Chemical and Physical Meteorology, 47*(5), 624–629. https://doi.org/10.3402/tellusb.v47i5.16077
Johnsen, S. J., Dahl-Jensen, D., Gundestrup, N., Steffensen, J. P., Clausen, H. B., Miller, H., Masson-Delmotte, V., Sveinbjörnsdottir, A. E., & White, J. (2001). Oxygen isotope and palaeotemperature records from six Greenland ice-core stations: Camp Century, Dye-3, GRIP, GISP2, Renland and NorthGRIP. *Journal of Quaternary Science*, *16*(4), 299–307. https://doi.org/10.1002/jqs.622
Johnsen, S. J., Dansgaard, W., & White, J. W. C. (1989). The origin of Arctic precipitation under present and glacial conditions. *Tellus B: Chemical and Physical Meteorology*, *41*(4), 452-468. https://doi.org/10.3402/tellusb.v41i4.15100
Johnsen, S. J. (1977). Stable isotope homogenization of polar firn and ice. In *Proc. of Symp. on Isotopes and Impurities in Snow and Ice* (pp. 210–219). International Association of Hydrological Sciences.
Jones, T. R., Cuffey, K. M., Roberts, W. H. G., Markle, B. R., Steig, E. J., Stevens, C. M., Valdes, P. J., Fudge, T. J., Sigl, M., Hughes, A. G., Morris, V., Vaughn, B. H., Garland, J., Vinther, B. M., Rozmiarek, K. S., Brashear, C. A., & White, J. W. C. (2023). Seasonal temperatures in West Antarctica during the Holocene. *Nature*, *613*(7943), 292–297. https://doi.org/10.1038/s41586-022-05411-8
Jones, T. R., Cuffey, K. M., White, J. W. C., Steig, E. J., Buizert, C., Markle, B. R., McConnell, J. R., & Sigl, M. (2017). Water isotope diffusion in the WAIS Divide ice core during the Holocene and last glacial. *Journal of Geophysical Research: Earth Surface*, *122*(1), 290–309. https://doi.org/10.1002/2016JF003938
Jones, T. R., Roberts, W. H. G., Steig, E. J., Cuffey, K. M., Markle, B. R., & White, J. W. C. (2018). Southern Hemisphere climate variability forced by Northern Hemisphere ice-sheet topography. *Nature*, *554*(7692), 351–355. https://doi.org/10.1038/nature24669
Jones, T. R., White, J. W. C., Steig, E. J., Vaughn, B. H., Morris, V., Gkinis, V., Markle, B. R., & Schoenemann, S. W. (2017). Improved methodologies for continuous-flow analysis of stable water isotopes in ice cores. *Atmospheric Measurement Techniques*, *10*(2), 617–632. https://doi.org/10.5194/amt-10-617-2017
Jouzel, J., Lorius, C., Petit, J. R., Genthon, C., Barkov, N. I., Kotlyakov, V. M., & Petrov, V. M. (1987). Vostok ice core: A continuous isotope temperature record over the last climatic cycle (160,000 years). *Nature, 329*(6138), 403–408. https://doi.org/10.1038/329403a0

Jouzel, J. (2013). A brief history of ice core science over the last 50 yr. *Climate of the Past*, *9*(6), 2525–2547. https://doi.org/10.5194/cp-9-2525-2013

Kelley, J. J., Stanford, K., Koci, B., Wumkes, M., & Zagorodnov, V. (1994). Ice coring and drilling technologies developed by the Polar Ice Coring Office. *Memoirs of National Institute of Polar Research. Special issue, 49*, 24-40.

Knutti, R., Flückiger, J., Stocker, T. F., & Timmermann, A. (2004). Strong hemispheric coupling of glacial climate through freshwater discharge and ocean circulation. *Nature*, *430*(7002), Article 7002. https://doi.org/10.1038/nature02786

Kunkel, K. E., Pielke, R. A., & Changnon, S. A. (1999). Temporal fluctuations in weather and climate extremes that cause economic and human health impacts: A review. *Bulletin of the American Meteorological Society, 80*(7), 1077–1098. https://doi.org/10.1175/1520-0477(1999)080<1077:TFIWAC>2.0.CO;2

Li, C., Battisti, D., & Bitz, C. (2010). Can North Atlantic Sea Ice Anomalies Account for Dansgaard-Oeschger Climate Signals? *Journal of Climate - J CLIMATE*, *23*, 5457–5475. https://doi.org/10.1175/2010JCLI3409.1

Li, C., Battisti, D. S., Schrag, D. P., & Tziperman, E. (2005). Abrupt climate shifts in Greenland due to displacements of the sea ice edge: GREENLAND CLIMATE SHIFTS AND SEA ICE. *Geophysical Research Letters*, *32*(19), n/a-n/a. https://doi.org/10.1029/2005GL023492

Markle, B. R., Steig, E. J., Roe, G. H., Winckler, G., & McConnell, J. R. (2018). Concomitant variability in high-latitude aerosols, water isotopes and the hydrologic cycle. *Nature Geoscience*, *11*(11), 853–859. https://doi.org/10.1038/s41561-018-0210-9

Masson-Delmotte, V., Buiron, D., Ekaykin, A., Frezzotti, M., Gallée, H., Jouzel, J., Krinner, G., Landais, A., Motoyama, H., Oerter, H., Pol, K., Pollard, D., Ritz, C., Schlosser, E., Sime, L. C., Sodemann, H., Stenni, B., Uemura, R., & Vimeux, F. (2011). A comparison of the present and last interglacial periods in six Antarctic ice cores. *Climate of the Past*, *7*(2), 397–423. https://doi.org/10.5194/cp-7-397-2011

Merlivat, L., & Jouzel, J. (1979). Global climatic interpretation of the deuterium‐oxygen 18 relationship for precipitation. *Journal of Geophysical Research: Oceans*, *84*(C8), 5029-5033.

Milankovitch, M. (1941). Kanon der Erdebestrahlung und seine Anwendung auf das Eiszeitenproblem. Königlich Serbische Akademie.

Mojtabavi, S., Wilhelms, F., Cook, E., Davies, S. M., Sinnl, G., Skov Jensen, M., Dahl-Jensen, D., Svensson, A., Vinther, B. M., Kipfstuhl, S., Jones, G., Karlsson, N. B., Faria, S. H., Gkinis, V., Kjær, H. A., Erhardt, T., Berben, S. M. P., Nisancioglu, K. H., Koldtoft, I., & Rasmussen, S. O. (2020). A first chronology for the East Greenland Ice-core Project (EGRIP) over the Holocene and last glacial termination. *Climate of the Past*, *16*(6), 2359–2380. https://doi.org/10.5194/cp-16-2359-2020

Montanari, A., Bahr, J., Blöschl, G., Cai, X., Mackay, D. S., Michalak, A. M., Rajaram, H., & Sander, G. (2015). Fifty years of *Water Resources Research*: Legacy and perspectives for the science of hydrology. *Water Resources Research, 51*(9), 6797–6803. https://doi.org/10.1002/2015WR017998

Pagano, T., & Sorooshian, S. (2002). Hydrologic cycle. In *Encyclopedia of Global Environmental Change* (Vol. 1, pp. 450–464). John Wiley & Sons, Ltd.

Peltier, W. R., & Vettoretti, G. (2014). Dansgaard-Oeschger oscillations predicted in a comprehensive model of glacial climate: A “kicked” salt oscillator in the Atlantic. *Geophysical Research Letters*, *41*(20), 7306–7313. https://doi.org/10.1002/2014GL061413

Percival, D. B., & Walden, A. T. (1993). Deterministic Spectral Analysis. In *Spectral Analysis for Physical Applications* (pp. 56–125). chapter, Cambridge: Cambridge University Press.

Petersen, S. V., Schrag, D. P., & Clark, P. U. (2013). A new mechanism for Dansgaard-Oeschger cycles. *Paleoceanography*, *28*(1), 24–30. https://doi.org/10.1029/2012PA002364

Pfahl, S., & Sodemann, H. (2014). What controls deuterium excess in global precipitation? *Climate of the Past*, 10(2), 771–781. https://doi.org/10.5194/cp-10-771-2014

Pfahl, S., & Wernli, H. (2008). Air parcel trajectory analysis of stable isotopes in water vapor in the eastern Mediterranean. *Journal of Geophysical Research: Atmospheres, 113*(D20). https://doi.org/10.1029/2008JD009839

Pratap, S., & Markonis, Y. (2022). The response of the hydrological cycle to temperature changes in recent and distant climatic history. *Progress in Earth and Planetary Science*, *9*(1), 30. https://doi.org/10.1186/s40645-022-00489-0

Rasmussen, S. O., Bigler, M., Blockley, S. P., Blunier, T., Buchardt, S. L., Clausen, H. B., Cvijanovic, I., Dahl-Jensen, D., Johnsen, S. J., Fischer, H., Gkinis, V., Guillevic, M., Hoek, W. Z., Lowe, J. J., Pedro, J. B., Popp, T., Seierstad, I. K., Steffensen, J. P., Svensson, A. M., … Winstrup, M. (2014). A stratigraphic framework for abrupt climatic changes during the Last Glacial period based on three synchronized Greenland ice-core records: Refining and extending the INTIMATE event stratigraphy. *Quaternary Science Reviews*, *106*, 14–28. https://doi.org/10.1016/j.quascirev.2014.09.007

Rasmussen, T. L., Thomsen, E., & Moros, M. (2016). North Atlantic warming during Dansgaard-Oeschger events synchronous with Antarctic warming and out-of-phase with Greenland Climate. Scientific Reports, 6(1). https://doi.org/10.1038/srep20535

Rayleigh, L. (1896). Theoretical considerations respecting the separation of gases by diffusion and similar processes. *The London, Edinburgh, and Dublin Philosophical Magazine and Journal of Science*, 42(259), 493-498.

Ronghui, H., & Yifang, W. (1989). The influence of ENSO on the summer climate change in China and its mechanism. *Advances in Atmospheric Sciences*, *6*(1), 21–32. https://doi.org/10.1007/BF02656915

Ruth, U., Barbante, C., Bigler, M., Delmonte, B., Fischer, H., Gabrielli, P., Gaspari, V., Kaufmann, P., Lambert, F., Maggi, V., Marino, F., Petit, J.-R., Udisti, R., Wagenbach, D., Wegner, A., & Wolff, E. W. (2008). Proxies and Measurement Techniques for Mineral Dust in Antarctic Ice Cores. *Environmental Science & Technology*, *42*(15), 5675–5681. https://doi.org/10.1021/es703078z

Seierstad, I. K., Abbott, P. M., Bigler, M., Blunier, T., Bourne, A. J., Brook, E., Buchardt, S. L., Buizert, C., Clausen, H. B., Cook, E., Dahl-Jensen, D., Davies, S. M., Guillevic, M., Johnsen,

S. J., Pedersen, D. S., Popp, T. J., Rasmussen, S. O., Severinghaus, J. P., Svensson, A., & Vinther, B. M. (2014). Consistently dated records from the Greenland GRIP, GISP2 and NGRIP ice cores for the past 104 ka reveal regional millennial-scale δ18O gradients with possible Heinrich event imprint. *Quaternary Science Reviews*, *106*, 29–46. https://doi.org/10.1016/j.quascirev.2014.10.032

Steen-Larsen, H. C., Johnsen, S. J., Masson-Delmotte, V., Stenni, B., Risi, C., Sodemann, H., Balslev-Clausen, D., Blunier, T., Dahl-Jensen, D., Ellehøj, M. D., Falourd, S., Grindsted, A., Gkinis, V., Jouzel, J., Popp, T., Sheldon, S., Simonsen, S. B., Sjolte, J., Steffensen, J. P., … White, J. W. C. (2013). Continuous monitoring of summer surface water vapor isotopic composition above the Greenland Ice Sheet. *Atmospheric Chemistry and Physics*, *13*(9), 4815–4828. https://doi.org/10.5194/acp-13-4815-2013

Steen-Larsen, H. C., Masson-Delmotte, V., Hirabayashi, M., Winkler, R., Satow, K., Prié, F., Bayou, N., Brun, E., Cuffey, K. M., Dahl-Jensen, D., Dumont, M., Guillevic, M., Kipfstuhl, S., Landais, A., Popp, T., Risi, C., Steffen, K., Stenni, B., & Sveinbjörnsdottír, A. E. (2014). What controls the isotopic composition of Greenland surface snow? *Climate of the Past*, *10*(1), 377–392. https://doi.org/10.5194/cp-10-377-2014

Steen-Larsen, H. C., Sveinbjörnsdottir, A. E., Jonsson, Th., Ritter, F., Bonne, J.-L., Masson-Delmotte, V., Sodemann, H., Blunier, T., Dahl-Jensen, D., & Vinther, B. M. (2015). Moisture sources and synoptic to seasonal variability of North Atlantic water vapor isotopic composition. *Journal of Geophysical Research: Atmospheres*, *120*(12), 5757–5774. https://doi.org/10.1002/2015JD023234

Stocker, T. F., & Johnsen, S. J. (2003). A minimum thermodynamic model for the bipolar seesaw. *Paleoceanography, 18*(4). https://doi.org/10.1029/2003PA000920

Svensson, A., Andersen, K. K., Bigler, M., Clausen, H. B., Dahl-Jensen, D., Davies, S. M., Johnsen, S. J., Muscheler, R., Parrenin, F., Rasmussen, S. O., Rothlisberger, R., Seierstad, I., Steffensen, J. P., & Vinther, B. M. (2008). A 60 000 year Greenland stratigraphic ice core chronology. *Clim. Past*, 11.

Thompson, L. G., & Mosley-Thompson, E. (1981). Microparticle Concentration Variations Linked with Climatic Change: Evidence from Polar Ice Cores. *Science*, *212*(4496), 812–815. https://doi.org/10.1126/science.212.4496.812

Timmermann, A., An, S.-I., Kug, J.-S., Jin, F.-F., Cai, W., Capotondi, A., Cobb, K. M., Lengaigne, M., McPhaden, M. J., Stuecker, M. F., Stein, K., Wittenberg, A. T., Yun, K.-S., Bayr, T., Chen, H.-C., Chikamoto, Y., Dewitte, B., Dommenget, D., Grothe, P., … Zhang, X. (2018). El Niño–Southern Oscillation complexity. *Nature*, *559*(7715), 535–545. https://doi.org/10.1038/s41586-018-0252-6

Vaughn, B., Morris, V., Nunn, R., Jones, T., Brashear, C., Rozmiarek, K., Hughes, A., Skorski, W., Born, A., Buizert, C., Dahl-Jensen, D., Gkinis, V., Holme, C., Johnsen, S., Jensen, M., Kjellman, S., Langebroek, P., Mekhaldi, F., Nisancioglu, K. H., Quistgaard, T., Rheinlænder, J., Rasmussen, S. O., Simon, M., Sinnl, G., Sowers, T., Steen-Larsen, H. C., Steffensen, J. P., Skorski, W., Vinther, B., Wong, J., & White, J. (2022). EGRIP water isotope data 21.5 m to

2120.7 m depth at 5 cm resolution, from continuous flow analysis (CFA). Arctic Data Center. https://doi.org/10.18739/A2H41JP05

Wang, Z., Zhang, X., Guan, Z., Sun, B., Yang, X., & Liu, C. (2015). An atmospheric origin of the multi-decadal bipolar seesaw. Scientific Reports, 5(1). https://doi.org/10.1038/srep08909

Weiss, H., Courty, M. A., Wetterstrom, W., Guichard, F., Senior, L., Meadow, R., & Curnow, A. (1993). The genesis and collapse of third millennium north Mesopotamian civilization. SCIENCE-NEW YORK THEN WASHINGTON-, 261, 995-995.

Whillans, I. M., & Grootes, P. M. (1985). Isotopic diffusion in cold snow and firn. *Journal of Geophysical Research: Atmospheres,* 90(D2), 3910–3918. https://doi.org/10.1029/JD090iD02p03910

Wright, L. E. (2022). Oxygen isotopes. In Encyclopedia of Geoarchaeology (pp. 1-7). Cham: Springer International Publishing.

Yang, D., Yang, Y., & Xia, J. (2021). Hydrological cycle and water resources in a changing world: A review. *Geography and Sustainability*, *2*(2), 115–122. https://doi.org/10.1016/j.geosus.2021.05.003